Journal of Human Evolution 121 (2018) 235–253

Contents lists available at ScienceDirect

Journal of Human Evolution

journal homepage: www.elsevier.com/locate/jhevol

Who were the Nataruk people? Mandibular morphology among late Pleistocene and early Holocene fisher-forager populations of West Turkana (Kenya)

Aurélien Mounier [a, b, **], Maria Correia [b], Frances Rivera [b], Federica Crivellaro [b], Ronika Power [b, c], Joe Jeffery [b], Alex Wilshaw [b], Robert A. Foley [b, d], Marta Mirazón Lahr [b, d, *]

[a] UMR 7194, CNRS-Muséum National D'Histoire Naturelle, Musée de L'Homme, 17 Place Du Trocadéro et Du 11 Novembre, 75016 Paris, France
[b] Leverhulme Centre for Human Evolutionary Studies, Department of Archaeology, University of Cambridge, Fitzwilliam Street, Cambridge CB2 1QH, United Kingdom
[c] Department of Ancient History, Level 5, W6A Building, Macquarie University, NSW 2109, Australia
[d] Turkana Basin Institute, Kenya

ARTICLE INFO

Article history:
Received 17 July 2017
Accepted 25 April 2018
Available online 29 May 2018

Keywords:
Late human evolution
Africa
Nataruk
West-Turkana
Mandibles
Phenetic

ABSTRACT

Africa is the birthplace of the species *Homo sapiens*, and Africans today are genetically more diverse than other populations of the world. However, the processes that underpinned the evolution of African populations remain largely obscure. Only a handful of late Pleistocene African fossils (~50-12 Ka) are known, while the more numerous sites with human fossils of early Holocene age are patchily distributed. In particular, late Pleistocene and early Holocene human diversity in Eastern Africa remains little studied, precluding any analysis of the potential factors that shaped human diversity in the region, and more broadly throughout the continent. These periods include the Last Glacial Maximum (LGM), a moment of extreme aridity in Africa that caused the fragmentation of population ranges and localised extinctions, as well as the 'African Humid Period', a moment of abrupt climate change and enhanced connectivity throughout Africa. East Africa, with its range of environments, may have acted as a refugium during the LGM, and may have played a critical biogeographic role during the heterogene`ous environmental recovery that followed. This environmental context raises a number of questions about the relationships among early Holocene African populations, and about the role played by East Africa in shaping late hunter-gatherer biological diversity. Here, we describe eight mandibles from Nataruk, an early Holocene site (~10 Ka) in West Turkana, offering the opportunity of exploring population diversity in Africa at the height of the 'African Humid Period'. We use 3D geometric morphometric techniques to analyze the phenotypic variation of a large mandibular sample. Our results show that (i) the Nataruk mandibles are most similar to other African hunter-fisher-gatherer populations, especially to the fossils from Lothagam, another West Turkana locality, and to other early Holocene fossils from the Central Rift Valley (Kenya); and (ii) a phylogenetic connection may have existed between these Eastern African populations and some Nile Valley and Maghrebian groups, who lived at a time when a Green Sahara may have allowed substantial contact, and potential gene flow, across a vast expanse of Northern and Eastern Africa.
© 2018 Elsevier Ltd. All rights reserved.

1. Introduction

Africa is the birthplace of our species, *Homo sapiens*, from where all human populations diversified. The earliest fossils that show the unique, universal characteristics of a modern human morphology are found in East Africa 200,000–160,000 years ago (Ka) (Day, 1969; Leakey, 1969; White et al., 2003; Fleagle et al., 2008), while recent proposals for an earlier origin for the species would extend this date to ca. 300 Ka (Hublin et al., 2017). Africans today are genetically more diverse than other populations of the world, reflecting the population size and time-depth of modern human presence in the continent (Liu et al., 2006; Li et al., 2008). Genetic data further point to significant population change associated with

* Corresponding author.
** Corresponding author.
E-mail addresses: aurelien.mounier@mnhn.fr (A. Mounier), mbml1@cam.ac.uk (M. Mirazón Lahr).

https://doi.org/10.1016/j.jhevol.2018.04.013
0047-2484/© 2018 Elsevier Ltd. All rights reserved.

the expansion of food-producing populations in the last 4000 years (Tishkoff et al., 2009). However, between these two extremes in time, the historical, ecological and adaptive processes that underpinned the evolution of African populations remain largely unknown. Only a handful of late Pleistocene sites (~50-12 Ka) with human remains are known (Grine, 2016), and these are mostly located in North or South Africa. This period includes the Last Glacial Maximum, a moment of extreme aridity in Africa (Gasse, 2000; Clark et al., 2009) that caused the fragmentation of population ranges and localised extinctions. East Africa, with its diversity of environments and high relief, may have acted as a refugium (Mirazón Lahr and Foley, 2016), thus playing a critical biogeographic role within the continent during phases of late Pleistocene aridity. Contrastingly, the early-to-mid Holocene (12-5 Ka) – the 'African Humid Period' (AHP) – was a moment of abrupt climate change (de Menocal et al., 2000) and enhanced connectivity throughout Africa, including the expansion of productive biomes and greening of the Sahara (Larrasoaña et al., 2013). However, the timing of environmental recovery was not synchronous throughout the continent (Carolin et al., 2013), creating the opportunity for the differential expansion of those populations who first experienced ameliorated conditions (Mirazón Lahr, 2016). This environmental context raises a number of questions about the relationships among early Holocene African populations and, in particular, about the role played by East Africa in shaping late hunter-gatherer biological diversity in the continent. The number of sites and human fossil remains of early Holocene age in Africa is greater than earlier phases, but these are patchily distributed. In particular, the late Pleistocene and early Holocene human diversity of Eastern Africa is still poorly known, precluding any analysis of the potential factors that shaped human diversity in the region, and more broadly throughout the continent.

This paper describes the variation and affinities of a new group of fossil mandibles from the site of Nataruk in West Turkana, Kenya, dating to ~10 Ka (Mirazón Lahr et al., 2016). In the context of a scarce African fossil record, the discovery in August 2012 of this new Kenyan site is important. Nataruk is located ~30 km southwest of Lake Turkana, and ~2 km from the paleoshore of Lake Turkana during the AHP. The site is at the Eastern edge of a small depression that would have formed a lagoon during periods of high precipitation, abutting small dunes rising ~4 m above the surface. Small-to medium-sized gravel, lying loosely over a layer of lake sediments, covers the surface of the ridge and mounds largely characterized by shell and carbonate deposits. The majority of the fragmentary faunal remains recovered are aquatic/lake-edge species. The site has been dated using radiocarbon from shells and sediment samples associated with the human remains, optical luminescence dating and uranium-series dates that yielded an age estimate of ~10.5–9.5 Ka (Mirazón Lahr et al., 2016). A minimum of 27 fossil individuals, among which 12 are represented by partially complete skeletons, were uncovered at Nataruk. Ten skeletons show evidence of human-inflicted trauma and the site was described as being the scene of inter-group conflict between hunter-fisher-gatherer groups and the earliest evidence of warfare (Mirazón Lahr et al., 2016). Most of the 12 articulated skeletons are reasonably well-preserved; however, the crania are broken or partly missing. For four specimens (KNM-WT 71258, 71259, 71260, and 71265), the skull is fragmentary; another four individuals lack most of the upper face (KNM-WT 71251, 71255, 71256 and 71263), KNM-WT 71253 lacks most of the occipital and basicranium, and KNM-WT 71254 preserves only the right parietal, the frontal and the right zygomatic. KNM-WT 71257 and 71264 skulls are almost complete, but their calvaria are deformed due to trauma. However, with the exception of KNM-WT 71258, 71259, 71260 and 71265, all the specimens have well-preserved mandibles that exhibit minimal traumatic lesions, although most mandibular condyles are missing; the right ascending ramus of KNM-WT 71254 has a linear perforation on its antero-lateral surface (Figs. 1 and 2, Table 2; Mirazón Lahr et al., 2016), but this lesion has not affected its overall shape. Therefore, while the cranial remains from Nataruk are either fragmentary or show evidence of violent trauma, which precludes unbiased morphometric study, the well-preserved mandibular remains offer the opportunity of exploring population diversity in Africa at the height of the 'African Humid Period'.

In this paper we examine the phenotypic variation of the people of Nataruk in order to understand their phenetic affinities with worldwide populations, and, more specifically with African populations. The population affinities of the people of Nataruk have not been explored before, although our expectation is that they will show a close relationship to neighboring fisher-forager groups from the early Holocene of Turkana, and more broadly, to early Holocene eastern African forager groups. While this hypothesis is based on the spatial and temporal proximity that would have promoted the connectivity among these groups, the potential relationships of the Nataruk population to other African populations is unmapped. Thus, this paper aims to test both this hypothesis and describe the broad phenetic relationships among some Holocene African populations, both of which depend on the presence of a signal of population history in mandibular morphology.

1.1. The mandible as a source of evolutionary information

The human cranium is often used to reconstruct morphological and phylogenetic affinities among populations and species because variation in its morphology is largely explained by a model of neutral evolution, i.e., the result of stochastic processes of mutation and genetic drift (Roseman and Weaver, 2004; Nicholson and Harvati, 2006; Smith, 2009; von Cramon-Taubadel, 2009a; Betti et al., 2010; Galland, 2013; Katz et al., 2017). However, skull morphology must still be compatible with a number of different functions. These include protection of the brain and sensory organs, food processing and maintenance of the respiratory airways (Daegling, 2010). As a consequence, certain regions of the skull also reflect those functions and the external factors that influence them, to different degrees (von Cramon-Taubadel, 2014; Noback and Harvati, 2015b). Notably, it has been suggested that the upper face – especially the nasal cavity (Noback et al., 2011; Zaidi et al., 2017) – is influenced by climate, while the mandible together with general cranial shape might be more influenced by diet (Harvati and Weaver, 2006; Smith, 2009; von Cramon-Taubadel, 2009b, 2011; Noback and Harvati, 2015a). Nevertheless, such shape differences associated with climatic (Zaidi et al., 2017) and dietary pressures (Katz et al., 2017) are relatively small, most strongly expressed at the extremes of the adaptive range (i.e., among populations who live in very extreme environments), and overlap between populations is considerable, indicating that the impact of these factors on skull morphology may be less significant than previously hypothesised.

A recent study by Katz et al. (2017) suggests that the phenotypic differences due to diet in both mandible and cranium tend to be smaller than typical differences between sexes, groups of average relatedness and between individuals, further indicating that differences attributable to subsistence strategy may appear somewhat magnified when comparing populations which are closely related. The study, nevertheless, points towards modest directional shape differences between foragers and farmers, as has been advocated before (see von Cramon-Taubadel, 2011). This can be explained by a decrease in masticatory stress associated with the transition from tougher or harder foraged foods to tender or soft processed agricultural ones (González-José et al., 2005; Lieberman, 2008; von

Figure 1. Four of the mandibles from the site of Nataruk (West Turkana, Kenya) showed in norma lateralis, norma facialis, norma occipitalis and normal superalis (from left to right). (A) KNM-WT 71251, (B) KNM-WT 71253, (C) KNM-WT 71254, (D) KNM-WT 71255. The mandibles are scaled in relation to each other.

Cramon-Taubadel, 2011; Noback and Harvati, 2015a; Katz et al., 2017). However, if the magnitude of shape difference induced by diet is relatively small, it may be assumed that neutral evolution (i.e., genetic drift, gene flow reflecting population history) is the primary evolutionary process by which human cranial and mandibular phenotypic diversity has been shaped (Katz et al., 2017). Therefore, while discerning between the contributions of adaptation and plasticity to cranial and mandibular shape variation is complex, adult cranio-mandibular morphology does record evolutionary history and can be used to track population history. Its known sensitivity to environmental and lifestyle factors acting at different temporal scales, and expressed to different degrees in particular morphological regions of the skull and mandible, has, nevertheless, to be taken into account.

The present study uses mandibular morphology to assess the phenetic relationships of the Nataruk population, while discussing environmental and lifestyle factors that could have influenced the morphological diversity observed. We provide a complete morphological description of the eight best-preserved mandibles from Nataruk, as well as an assessment of their morphological variation using geometric morphometric techniques. We aim to quantify the morphological diversity observed in the Nataruk mandibles to clarify their affinity to other prehistoric and historic human populations both within and outside Africa.

2. Materials and methods

2.1. Materials

The study sample is composed of eight mandibles from Nataruk (Figs. 1 and 2, Tables 1 and 2; Mirazón Larrasoaña et al., 2013). The state of preservation of the sample is varied, but all individuals included preserve the mandibular body and at least most of one of its mandibular rami. In order to assess the morphological variability and affinity of the Nataruk mandibular sample, we compared these specimens to a sample of 304 adult modern human mandibles. The comparative sample, listed by population (Table 1) and by sites in case of fossils (Table 2) was chosen to cover a wide range of chronological and spatial variation. Chronologically, the range incorporates examples from the late Pleistocene (100 – 12 Ka, $n = 49$), early Holocene (12 – 6 Ka, $n = 14$), late Holocene (6 – 2 Ka, $n = 63$) and 19th and 20th centuries ($n = 178$); geographically, the specimens originate from sub-Saharan Africa ($n = 77$), North Africa ($n = 101$), continental Asia ($n = 12$), South Asia ($n = 31$), Europe ($n = 28$), Oceania ($n = 37$) and Greenland ($n = 18$). The recent European mandibles ($n = 17$) originate from England ($n = 10$) and from Eastern Europe ($n = 7$) in order to capture more of the European morphological variation. We selected a high percentage of African specimens, not

Figure 2. Four of the mandibles from the site of Nataruk (West Turkana, Kenya) showed in norma lateralis, norma facialis, norma occipitalis and normal superalis (from left to right). (A) KNM-WT 71256, (B) KNM-WT 71257, (C) KNM-WT 71263, (D) KNM-WT 71264. The mandibles are scaled in relation to each other. Norma lateralis is reversed for KNM-WT 71256.

only because Africa offers the best comparative framework with which to understand the morphological variation of the Nataruk population, but also because Africa shows the highest genetic diversity compared to other regions of the world and represents a wide range of adaptive niches. Additional information on the remainder of the comparative sample can be found in the Supplementary Online Material (SOM) Table S1.

The sample is estimated to be composed of 35.3% female and 64.7% male individuals (SOM Table S1). The sex was established from previous studies; however, for almost half of the sample (i.e., 47.11%), this information was lacking in the literature, and sex determination was established on the secondary sexual characteristics of the skull (see Buikstra and Ubelaker, 1994; White et al., 2011). The sex ratio (*n* females/*n* total *100) for each population is indicated in Table 1.

2.2. Methods

2.2.1. Morphological description The morphology of the eight Nataruk specimens is described in detail, and the main morphological features of the mandibles are analyzed in light of known morphologies generally considered to be specific to modern humans and Neandertals.

2.2.2. Geometric morphometric analyses Mandibular shape was captured through 54 landmarks (six medial and 24 bilateral landmarks) selected to maximize the characterization of the mandible's morphology while taking into consideration the state of preservation of the specimens. Missing landmarks were estimated by mirroring and, where mirroring was impossible, by a thin-plate-spline (i.e., TPS) interpolation using the available landmarks (Bookstein, 1989). In order to evaluate the performance of TPS in estimating the missing landmarks, we simulated missing landmarks on 30 complete cases and tested the averages and variances of the simulated imputations (SOM, Fig. S1). To correct for bilateral asymmetry in each specimen, the right and left configurations were scaled to unit centroid size, before being aligned using a Generalized Procrustes Analysis (i.e., GPA, see Gower, 1975; Rohlf and Slice, 1990) and rescaled to their original size. The mean coordinates, based on a total of 30 landmarks per specimens (SOM Table S2, Fig. 4), were used to perform the subsequent analyses on the mandibles.

Each landmark data set was then superimposed using a GPA, which allows for the isolation of the size (i.e., centroid size) from the shape component (i.e., Procrustes residuals). The two variables can be analyzed independently to identify phenetic signals in the data.

Table 1
Specimens used in the study.

Meta-populations and Populations	*n*	Sex ratio[a]	Provenance	Chronology	Reference (chronology)
Nataruk	8	0.36	Kenya	10,500–9500 BP	(Mirazón Lahr et al., 2016)
Extant Sub-Sahara (n = 63)					
Haya	24	0.33	Tanzania	19th century	–
Somali	18	0.11	Somalia	20th century	–
Daarod (14); Ainhao (2); Hahr Jalo (2)					
Khoisan	11	0.54	South Africa	19th century	–
Bantu	10	0	South Africa	19th century	–
Extant Asia (n = 43)					
Andamanese	11	0.54	Andaman Islands, India	19th century	–
Nicobarese	11	0.45	Nicobar Islands, India	19th century	–
Chinese	12	0.1	China	19th century	–
Sri Lankan	9	0.22	Sri Lanka	19th century	–
Veddah (4); Singhalese (3); Tamil (2)					
Extant Oceania (n = 37)					
Papuan	16	0.38	Papua New Guinea	19th century	–
Australian	21	0.43	Australia	19th century	–
Extant European (n = 17)					
European	17	0.47	Europe	19th century	–
Extant Inuit (n = 18)					
Inuit	18	0.4	Greenland	19th century	–
Nile Valley (n = 63)					
Kerma (Nubian)	16	0.5	Sudan	3750–3480 BP	(Collett, 1933; Simon, 1989)
Jebel Moya (Nubian)	14	0.57	Sudan	5000–2100 BP	(Brass and Schwenniger, 2013)
Badari (Pre-Dynastic)	18	0.39	Egypt	5440–5110 BP	(Hendrickx, 1999)
Naqada (Pre-Dynastic)	15	0.47	Egypt	5000–4000 BP	(Hendrickx, 1999)
Holocene Kenya (n = 14)					
Lothagam	7	0.43	Kenya	9000–6000 BP	(Robbins, 1974)
Central Rift[b]	7	0.29	Kenya	8210–5000 BP	–[c]
Pleistocene North Africa (n = 38)					
Taforalt – Grotte des Pigeons	20	0.35	Morocco	15,000–10,000 BP	(Aoudia-Chouakri, 2013)
Afalou Bou Rhummel	17	0.12	Algeria	15,000–11,000 BP	(Aoudia-Chouakri, 2013)
Nazlet Khater 2	**1**	**0**	**Egypt**	**35,000 BP**	**(Crevecoeur, 2006)**
Pleistocene Europe (n = 11)					
Europe[b]	11	0.5	–	50,000–12,000 BP	–[c]
Total	**312**	**0.35**			

Bold type indicates that the original fossils were examined.
[a] The sex ratio corresponds to the number of females divided by the total number of specimens per population.
[b] Individual fossil specimens that compose this sample are listed in Table 2.
[c] References for chronology are listed in Table 2.

2.2.3. Statistical analyses To explore the patterns of morphological variation within the mandibular sample, and to decipher the phenetic affinities of the Nataruk mandibles, we ran three different sets of analyses. Firstly, an analysis of size variation, represented by the centroid size extracted from the GPA; secondly, an analysis of shape variation, represented by the Procrustes residuals and the principal components obtained after between groups principal components analyses (i.e., bgPCA), and finally, phenograms were built using a neighbor-joining algorithm (Saitou and Nei, 1987) based on Euclidian distances calculated from shape data. All analyses were run from the same database organized in different groups. First, we analyzed the 23 worldwide populations of the database, we then analyzed 10 meta-populations which regroup some of the previous populations within geochronological coherent categories, and finally, we focused on the African sample only, considering both extant and prehistoric samples (Tables 1 and 2).

To visualize the difference in size between the groups, we built boxplots using the centroid size (Table 3) extracted from the results of the GPA (Fig. 3).

The shape variation within the sample was explored using bgPCA based on the Procrustes residuals (Figs. 4–6, SOM Table S3). The bgPCA tests the significance of the between group distances (Tables 4–6). We used the worldwide populations, meta-populations and the African populations as group variables.

Finally, in order to infer the biological affinity and population history of the Nataruk mandibles, we built neighbor-joining phenograms (Fig. 7) using all PCs from PCAs (SOM Table S4) run on population mean shapes to compute Euclidean distances. Ten thousand bootstrap replications were run on the obtained phenograms in order to test for the stability of tree topology.

All analyses were performed on the R platform using the Morpho (version 2.1; Schlager, 2013) and Geomorph (version 2.1.2; Adams and Otárola-Castillo, 2013) packages for the 3D geometric morphometric analyses, the Ade4 (version 1.7–4; Dray and Dufour, 2007) package for the bgPCA, and the Phangorn package (Schliep, 2011) for the neighbor-joining analyses.

3. Results

3.1. Morphological description

The Nataruk mandibles are large and strongly built as exemplified by their centroid size (see Centroid size below), which is, on average, larger than the other meta-populations of the comparative sample (Table 3). Additionally, they show wide rami and mandibular corpora (Figs. 1 and 2).

On the symphyseal region, we note a strongly developed mentum osseum in most of the specimens showing the characteristic modern human inverted 'T' chin (Schwartz and Tattersall, 2000). The mentum osseum is slightly less salient on KNM-WT 71263 (Fig. 2C), but this may be due to the cracks on the anterior surface of the symphyseal region of this specimen. It is important to note that the 3 females of the Nataruk sample show a strongly developed and projecting mentum osseum. The alveolar region is

Table 2
Description of fossil specimens.

Specimen	Sex	Site	Chronology	Chronology references
Holocene		*Nataruk*		
KNM-WT 71251	M	Nataruk, West Turkana, Kenya	10,500–9500 BP	(Mirazón Lahr et al., 2016)
KNM-WT 71253	M	Nataruk, West Turkana, Kenya	10,500–9500 BP	(Mirazón Lahr et al., 2016)
KNM-WT 71254	F?	Nataruk, West Turkana, Kenya	10,500–9500 BP	(Mirazón Lahr et al., 2016)
KNM-WT 71255	F	Nataruk, West Turkana, Kenya	10,500–9500 BP	(Mirazón Lahr et al., 2016)
KNM-WT 71256	F	Nataruk, West Turkana, Kenya	10,500–9500 BP	(Mirazón Lahr et al., 2016)
KNM-WT 71257	M	Nataruk, West Turkana, Kenya	10,500–9500 BP	(Mirazón Lahr et al., 2016)
KNM-WT 71263	M	Nataruk, West Turkana, Kenya	10,500–9500 BP	(Mirazón Lahr et al., 2016)
KNM-WT 71264	M	Nataruk, West Turkana, Kenya	10,500–9500 BP	(Mirazón Lahr et al., 2016)
		Lothagam		
KNM-LT 13702E	M?	Lothagam, West Turkana, Kenya	9000–6000 BP	(Robbins, 1974)
KNM-LT 13704B	M?	Lothagam, West Turkana, Kenya	9000–6000 BP	(Robbins, 1974)
KNM-LT 27710	M?	Lothagam, West Turkana, Kenya	9000–6000 BP	(Robbins, 1974)
KNM-LT 27712C	M?	Lothagam, West Turkana, Kenya	9000–6000 BP	(Robbins, 1974)
KNM-LT 27714	F?	Lothagam, West Turkana, Kenya	9000–6000 BP	(Robbins, 1974)
KNM-LT 27715B	F?	Lothagam, West Turkana, Kenya	9000–6000 BP	(Robbins, 1974)
KNM-LT 27717B	F?	Lothagam, West Turkana, Kenya	9000–6000 BP	(Robbins, 1974)
		Central Rift Valley		
Elmenteita A	M	Elmenteita, Bromhead, Kenya	7410 ± 160 BP	(Protsch, 1978)
Elmenteita D	M	Elmenteita, Bromhead, Kenya	7410 ± 160 BP	(Protsch, 1978)
Elmenteita F1	F	Elmenteita, Bromhead, Kenya	7410 ± 160 BP	(Protsch, 1978)
Gamble's Cave 4	M	Gamble's Cave, Kenya	8210 ± 260 BP	(Protsch, 1978)
Gamble's Cave 5	M	Gamble's Cave, Kenya	8210 ± 260 BP	(Protsch, 1978)
Nakuru IX	F	Nakuru, Kenya	Early Pastoral Neolithic	(Leakey, 1970)
Willey Kopje II	M	Willey Kopje, Kenya	Early Pastoral Neolithic	(Leakey, 1970)
Pleistocene		*Afalou*		
Afalou A.1	M	Afalou Bou Rhummel, Algeria	15,000–11,000 BP	(Aoudia-Chouakri, 2013)
Afalou A.2	M	Afalou Bou Rhummel, Algeria	15,000–11,000 BP	(Aoudia-Chouakri, 2013)
Afalou A.3	F	Afalou Bou Rhummel, Algeria	15,000–11,000 BP	(Aoudia-Chouakri, 2013)
Afalou A.5	F?	Afalou Bou Rhummel, Algeria	15,000–11,000 BP	(Aoudia-Chouakri, 2013)
Afalou A.10	M	Afalou Bou Rhummel, Algeria	15,000–11,000 BP	(Aoudia-Chouakri, 2013)
Afalou A.12	M?	Afalou Bou Rhummel, Algeria	15,000–11,000 BP	(Aoudia-Chouakri, 2013)
Afalou A.13	M	Afalou Bou Rhummel, Algeria	15,000–11,000 BP	(Aoudia-Chouakri, 2013)
Afalou A.14	M	Afalou Bou Rhummel, Algeria	15,000–11,000 BP	(Aoudia-Chouakri, 2013)
Afalou A.28	M	Afalou Bou Rhummel, Algeria	15,000–11,000 BP	(Aoudia-Chouakri, 2013)
Afalou A.30	M?	Afalou Bou Rhummel, Algeria	15,000–11,000 BP	(Aoudia-Chouakri, 2013)
Afalou A.34	M?	Afalou Bou Rhummel, Algeria	15,000–11,000 BP	(Aoudia-Chouakri, 2013)
Afalou A.46	M?	Afalou Bou Rhummel, Algeria	15,000–11,000 BP	(Aoudia-Chouakri, 2013)
Afalou A.47	M?	Afalou Bou Rhummel, Algeria	15,000–11,000 BP	(Aoudia-Chouakri, 2013)
Afalou A.48	M?	Afalou Bou Rhummel, Algeria	15,000–11,000 BP	(Aoudia-Chouakri, 2013)
Afalou A.49	M?	Afalou Bou Rhummel, Algeria	15,000–11,000 BP	(Aoudia-Chouakri, 2013)
Afalou B 4	M?	Afalou Bou Rhummel, Algeria	15,000–11,000 BP	(Aoudia-Chouakri, 2013)
Afalou Md 2–3	M?	Afalou Bou Rhummel, Algeria	15,000–11,000 BP	(Aoudia-Chouakri, 2013)
		Taforalt		
Taf I	F?	Taforalt, Grotte des Pigeons, Morocco	15,000–10,000 BP	(Aoudia-Chouakri, 2013)
Taf IX	M	Taforalt, Grotte des Pigeons, Morocco	15,000–10,000 BP	(Aoudia-Chouakri, 2013)
Taf VIII PB	M	Taforalt, Grotte des Pigeons, Morocco	15,000–10,000 BP	(Aoudia-Chouakri, 2013)
Taf XI-B.C2	M	Taforalt, Grotte des Pigeons, Morocco	15,000–10,000 BP	(Aoudia-Chouakri, 2013)
Taf XI-C1	M?	Taforalt, Grotte des Pigeons, Morocco	15,000–10,000 BP	(Aoudia-Chouakri, 2013)
Taf XII-C1	M	Taforalt, Grotte des Pigeons, Morocco	15,000–10,000 BP	(Aoudia-Chouakri, 2013)
Taf XIV	F?	Taforalt, Grotte des Pigeons, Morocco	15,000–10,000 BP	(Aoudia-Chouakri, 2013)
Taf XIX-C1	F?	Taforalt, Grotte des Pigeons, Morocco	15,000–10,000 BP	(Aoudia-Chouakri, 2013)
Taf XV-C2	M?	Taforalt, Grotte des Pigeons, Morocco	15,000–10,000 BP	(Aoudia-Chouakri, 2013)
Taf XV-C5	M	Taforalt, Grotte des Pigeons, Morocco	15,000–10,000 BP	(Aoudia-Chouakri, 2013)
Taf XVI-C2	F?	Taforalt, Grotte des Pigeons, Morocco	15,000–10,000 BP	(Aoudia-Chouakri, 2013)
Taf XVII-C2	F	Taforalt, Grotte des Pigeons, Morocco	15,000–10,000 BP	(Aoudia-Chouakri, 2013)
Taf XVIII	M?	Taforalt, Grotte des Pigeons, Morocco	15,000–10,000 BP	(Aoudia-Chouakri, 2013)
Taf XX-C1	M?	Taforalt, Grotte des Pigeons, Morocco	15,000–10,000 BP	(Aoudia-Chouakri, 2013)
Taf XX-C2	F?	Taforalt, Grotte des Pigeons, Morocco	15,000–10,000 BP	(Aoudia-Chouakri, 2013)
Taf XXI	M?	Taforalt, Grotte des Pigeons, Morocco	15,000–10,000 BP	(Aoudia-Chouakri, 2013)
Taf XXV-C3	F?	Taforalt, Grotte des Pigeons, Morocco	15,000–10,000 BP	(Aoudia-Chouakri, 2013)
Taf XXV.2	M?	Taforalt, Grotte des Pigeons, Morocco	15,000–10,000 BP	(Aoudia-Chouakri, 2013)
Taf XXVII-C1	M?	Taforalt, Grotte des Pigeons, Morocco	15,000–10,000 BP	(Aoudia-Chouakri, 2013)
Taf XXVII-C2	M	Taforalt, Grotte des Pigeons, Morocco	15,000–10,000 BP	(Aoudia-Chouakri, 2013)
		Europe		
Brno 3	F	Brno, Czech Republic	26,300 BP	(Smith, 1982)
Dolní Věstonice 3	F	Dolní Věstonice, Czech Republic	29,000–26,000 BP	(Trinkaus and Svoboda, 2006)
Dolní Věstonice 13	M	Dolní Věstonice, Czech Republic	29,000–26,000 BP	(Trinkaus and Svoboda, 2006)
Dolní Věstonice 15	M	Dolní Věstonice, Czech Republic	29,000–26,000 BP	(Trinkaus and Svoboda, 2006)
Pavlov I	M	Pavlov, Czech Republic	29,000–26,000 BP	(Weninger and Joris, 2004)
Předmostí 4	F	Předmostí, Czech Republic	26,000 BP	(Svoboda, 2008)
Předmostí 3	M	Předmostí, Czech Republic	26,000 BP	(Svoboda, 2008)
Abri Pataud 1	F	Abri Pataud, France	21,000 BP	(Bricker and Mellars, 1987)
Chancelade	M	Chancelade, France	17,000–12,000 BP	(Sonneville-Bordes, 1959)

Table 2 (*continued*)

Specimen	Sex	Site	Chronology	Chronology references
Kostenski 14	M	Kostenski-Borshchevo, Russia	38,700–36,200 BP	(Marom et al., 2012)
Oberkassel 2	F	Oberkassel, Germany	~12,000 BP	(Street et al., 2006)
		Nazlet Khater		
Nazlet Khater 2	M	Nazlet Khater, Egypt	35,000 BP	(Crevecoeur, 2006)

Bold type indicates that the original fossils were examined.

Table 3
Comparison of the centroid size for each meta-population and population of the study.

Meta-populations	Populations	Africans	Centroid Size			
			Mean	Max	Min	sd
Nataruk ($n = 8$)			250.85	258.81	228.37	13.05
Nile Valley ($n = 63$)			227.69	261.56	201.68	13.21
	Kerma ($n = 16$)		237.11	257.05	222.76	8.18
	Jebel Moya ($n = 14$)		230.46	261.56	202.98	16.28
	Naqada ($n = 15$)		226.32	250.17	202.32	10.74
	Badari ($n = 18$)		218.31	243.76	201.68	9.76
Sub-Saharan ($n = 63$)			233.06	260.76	196.63	13.32
	Haya ($n = 24$)		237.84	259.72	213.32	10.36
	Somali ($n = 18$)		232.74	244.98	206.62	9.48
	Khoisan ($n = 11$)		216.96	242.83	196.63	14.75
	Bantu ($n = 10$)		239.89	260.76	221.57	10.33
Asia ($n = 43$)			223.54	241.15	191.24	12.39
	China ($n = 12$)		234.20	241.16	221.45	5.76
	Sri Lanka ($n = 9$)		225.83	240.22	209.09	9.82
	Andaman ($n = 11$)		209.90	223.92	191.24	10.38
	Nicobar ($n = 11$)		223.67	236.01	203.35	8.84
Oceania ($n = 37$)			231.61	251.72	209.39	10.51
	Papua (n = 16)		230.21	251.72	216.01	11.89
	Australia ($n = 21$)		232.68	250.14	209.39	9.50
Europe ($n = 17$)			231.89	246.51	218.38	8.03
Inuit ($n = 18$)			233.59	249.51	209.72	9.01
Holocene Kenya ($n = 14$)			246.63	277.94	226.16	15.86
	Holocene Central Rift ($n = 7$)		238.66	261.07	226.17	11.85
	Elmenteita ($n = 3$)		240.80	261.07	226.16	18.12
	Gamble's Cave ($n = 2$)		231.02	233.69	228.35	3.78
	Nakuru IX		243.99	–	–	–
	Willey Kopje II		242.18	–	–	–
	Lothagam ($n = 7$)		254.60	277.95	231.26	16.01
Pleistocene Europe ($n = 11$)			233.194	252.56	215.51	13.57
Pleistocene North Africa ($n = 38$)			245.08	272.89	215.90	14.14
	Afalou ($n = 17$)		242.87	264.13	218.31	11.20
	Taforalt ($n = 20$)		246.37	272.89	215.90	16.43
	Nazlet Khater 2		256.92	–	–	–

strongly curved, with a well-marked incurvatio mandibulae, and the incisors project beyond the edge of the symphysis. This feature is less developed on the KNM-WT 71251 and KNM-WT 71256 fossils; however, KNM-WT 71251 is strongly distorted in this region, with the incisors being compressed antero-posteriorly, and KNM-WT 71256 lacks both the crowns of the incisors and some alveolar bone surrounding the missing 2nd left incisor root.

The upper and lower margins of the mandibular corpora diverge strongly towards the front. A mandibular corpus with parallel margins is more characteristic of older hominin fossils (Mounier et al., 2009). Additionally, the lower margin of the corpus displays a strongly marked inferior curvature. This character seems to relate to size, with larger mandibles having a more curved lower margin (see below and Fig. 6). On the lateral surface of the mandibular corpus, the mental foramen is positioned either at the level of the M1-P4 septum (KNM-WT 71251, 71254, 71257, 71264) or at the level of the P4 (KNM-WT 71253, 71255, 71256, 71263), which is positioned slightly backwards compared to most modern humans (Mounier et al., 2009). The prominentia lateralis is also positioned backwards, as it is found either under M2 (KNM-WT 71256 and 71263) or even at the M2-M3 level. A prominentia lateralis positioned under the third molar is often considered a Neandertal apomorphy (Mounier et al., 2009); however, it is also linked to the general dimensions of a specimen, and in large modern human mandibles such a morphology is not uncommon. In norma lateralis, there is no retromolar space between the third molar and the ascending ramus, but we note the presence of a rather large oblique retromolar surface on all the mandibles.

The ascending rami are relatively wide, and the projection of the anterior-most part of the ramus on the mandibular corpus accounts for almost half of the mandibular total length. The deepest point of the mandibular notch is generally positioned in a posterior position, which has been described as a Neandertal characteristic feature in the past (Rak et al., 2002). However, this configuration of the mandibular notch can be found in modern humans, and as is the case with the prominentia lateralis, it also seems to be related to the general size of the specimen (Mounier et al., 2009). The condyle and coronoid process are equally elevated in most specimens, with the exception of KNM-WT 71253 and 71254, in which the condyle is slightly higher than the coronoid process. The mandibular notch joins the condyle in a lateral position, as is usually the case in modern humans. The gonial angle is regular and strongly everted in almost all specimens (with the exception of KNM-WT 71254 and 71255 which are both females), indicating strong muscle attachments.

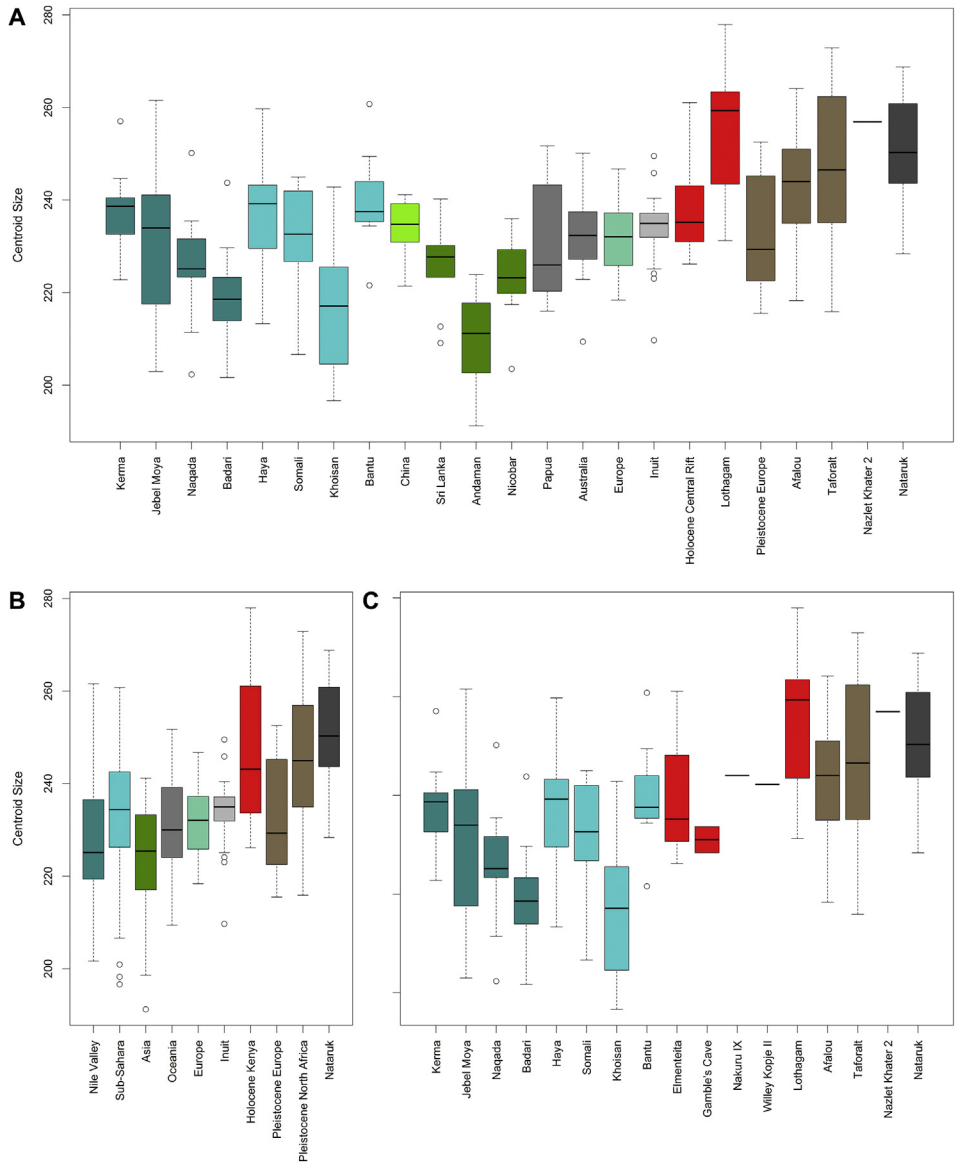

Figure 3. Boxplots showing centroid size according to the three different grouping of our sample. (A) worldwide populations, (B) worldwide meta-populations, and (C) African populations. The size of the Nataruk mandible is similar to Pleistocene specimens, and to the Lothagam sample.

The medial aspect of the mandible, unsurprisingly, does not display a planum alveolare. The mylohyoid line is well marked and usually inclined, with the exception of KNM-WT 71257 in which it is more diagonally orientated, a character that recalls the Neandertal morphology (Rosas, 1992; Creed-Miles et al., 1996). The mylohyoid line is positioned relatively low at the M3 level, except for KNM-WT 71251 and 71255; again, although this trait is observed in modern human mandibles (Mounier et al., 2009), it has been argued to be more common among Neandertals (Rosas, 1992; Creed-Miles et al., 1996).

In sum, the Nataruk mandibles, while having a very clear modern human morphological pattern, show a number of features that are common in other hominin species, such as the Neandertals. Such a phenotypic pattern has been described before in other early Holocene African populations, for instance the specimens from Assie-el-Habiod in Northern Mali (Dutour, 1989; Mounier et al., 2009) and Iwo Eleru in Nigeria (Harvati et al., 2011). However, most of the archaic morphological traits may be linked to size, which, in the case of Nataruk, is not surprising considering the large dimensions (see centroid size below) of the fossils.

3.2. Centroid size

A comparatively large average centroid size is one of the distinguishing features of the Nataruk mandibles. Here we compare the differences in centroid size between the populations and meta-populations of our sample (Table 3).

Figure 3 shows the distribution of the centroid size for each specimen according to their worldwide populations, meta-populations and within the African sample only. First, we note that the extant and pre-Dynastic populations are generally smaller than the early Holocene and Pleistocene specimens. The extant and pre-Dynastic specimens appear to have similar size with the exception of the gracile sub-Saharan Khoisan, the South-East Asian Andamanese Negritos, and, to a lesser extent, the pre-Dynastic Badari which are the smallest populations of our sample (Fig. 3A). Figure 3B shows that, when considered as meta-populations, there is virtually no size difference between the pre-Dynastic and recent populations. On the contrary, the Nataruk mandibles are in the higher range of size variation of our comparative sample in both cases. Their size is only matched by the late Pleistocene fossils from

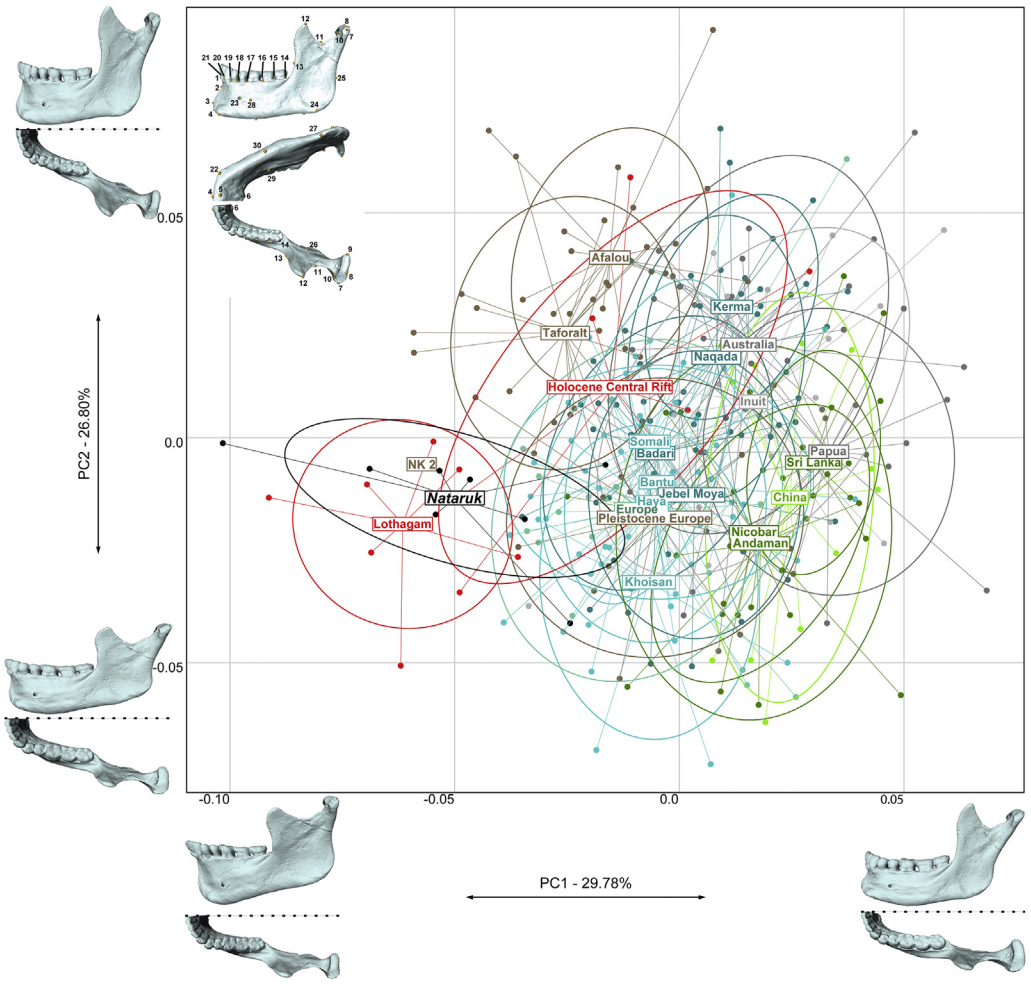

Figure 4. bgPCA showing the variation in shape within the mandibular sample grouped per worldwide populations. The ellipses represent the 90% confidence interval for the estimated distribution of the specimens of each population. Each specimen is linked to the centroid of its group of origin. The Nataruk specimens are closer in shape to the Lothagam (red) and late Pleistocene Afalou and Taforalt (brown) specimens. NK2 stands for Nazlet Khater 2. (For interpretation of the references to color in this figure legend, the reader is referred to the Web version of this article.)

North Africa (Afalou and Taforalt) and by the North African fossil Nazlet Khater 2. Most of the Holocene fossils from the Central Rift Valley (i.e., Elmenteita A, D and F1, Gamble's Cave 4 and 5, Nakuru IX and Wiley Kopje II) and the European Pleistocene specimens (i.e., Dolní Věstonice 3, XIII, XV, Pavlov I, Předmostí 4 and 3, Abri Pataud 1, Chancelade, Kostenski 14, Oberkassel 2) tend to be smaller than the North African fossils and Nataruk; they fit within the range of variation of the extant human sample. Finally, the mandibles from Lothagam appear to be slightly bigger than the Nataruk specimens, and the largest of the comparative sample. When looking at Figure 3C, we note that all of the Central Rift Holocene specimens, except one mandible from Elmenteita, are within the extant range of size variation while, again, the Nataruk specimens, along with Lothagam and the North African Pleistocene fossils, are larger.

3.3. Shape variation – between groups PCA

Figure 4 shows the first two bgPCs (56.58% of the total variance, SOM Table S3) of the bgPCA based on the Procrustes residuals of the analysis of the individual specimens grouped according to the 23 worldwide populations. Along bgPC1 (29.78% of the total variance) the shape deformation in the negative values represents a mandible with a strongly developed incurvatio mandibulae and mentum osseum, a deep mandibular body with margins that are strongly converging backwards, and a vertical wide and short ramus. On the positive side of the axis, the mandibular corpus is low with almost parallel margins, and the ramus is narrow and tall, making a wide open angle with the corpus. Additionally, the general length of the mandible increases along bgPC1. Along the second component (26.80% of the variance), the mandibular corpus and the mandibular ramus become thinner and more elongated; additionally, the general width of the mandible increases.

The dispersion of the cloud of points within the morphospace shows little separation among the comparative populations. We can, however, see that the Asian populations along with the Inuit, Papuan and, to a lesser extent, Australian specimens tend to share the morphospace represented by positive bgPC1 values; the Africans and Europeans are mainly positioned at the center of bgPC1, while the chronologically older samples (Afalou, Taforalt, Nazlet Khater 2, Holocene Central Rift and Lothagam) present negative values on bgPC1. It is worth noting that the Pleistocene specimens from Europe do not follow this pattern as they group at the centre of the chart with extant populations. Most populations are not discriminated along bgPC2, with the exception of the North African Pleistocene specimens (Afalou and Taforalt) from Nataruk and Lothagam samples. In more detail, the Nataruk specimens (black) are positioned at the margin of the main cloud of points, along with the Early Holocene specimens (red) from Lothagam and, to a lesser

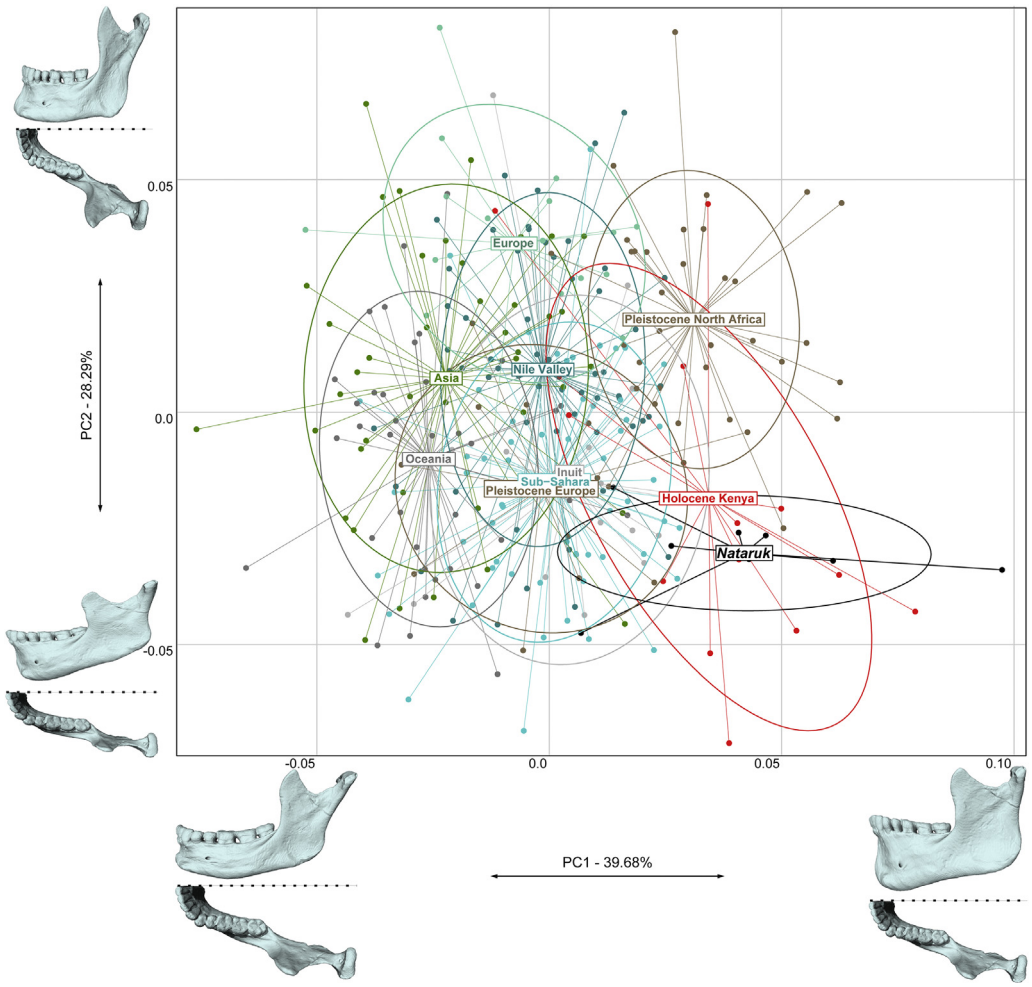

Figure 5. bgPCA showing the variation in shape within the mandibular sample grouped per worldwide meta-populations. The ellipses represent the 90% confidence interval for the estimated distribution of the specimens of each population. Each specimen is linked to the centroid of its group of origin. The Nataruk specimens are closer in shape to the Kenyan Holocene (red) and North Africa Pleistocene (brown) specimens. (For interpretation of the references to color in this figure legend, the reader is referred to the Web version of this article.)

extent, from the Central Rift. This last group displays, nevertheless, a much wider variation, as exemplified by the 90% confidence interval ellipse of the group which extends into the central part of the morphospace. The permutation test results run on the bgPCs (Table 4) indicate that, despite the overlap of most of the populations within the morphospace, the pairwise group differences are, in most cases, significant. The Nataruk specimens cannot be distinguished from Lothagam, the Holocene Central Rift specimens and from the Nazlet Khater 2 isolated fossil. Their morphology appears different from that of the other populations considered.

The second bgPCA was run between meta-populations, regrouping different populations into larger coherent geochronological groups. The first two bgPCs displayed in Figure 5 represent 67.97% of the total variance of the shape data (bgPC1: 39.68%; bgPC2: 28.29%). The mandibular shapes described are very similar to those of the first bgPCA, with reverse polarity along bgPC1, and an added general decrease in length of the mandible from negative to positive values, with mandibular corpus margins that become more parallel along bgPC2.

The morphospace (Fig. 5) displays a good separation between the means of each extant meta-population. BgPC1 separates individuals from Oceania and Asia from Africans and Europeans, while bgPC2 sets apart Europe, Asia and the North African Nile Valley specimens. Only the Inuit and sub-Saharan mandibles cannot be separated within the morphospace. The African early Holocene and Pleistocene samples present positive values on the first component, hence, occupying a different morphospace from the rest of the sample. This is not the case of the European Pleistocene specimens, which group around the Inuit and extant sub-Saharan African mandibles at the center of the chart. It is worth noting the difference in shape between extant and Pleistocene Europeans, the prehistoric sample being more similar to extant sub-Saharan African and Inuit specimens than to current Europeans. The second component separates Nataruk and most of the early Holocene Kenyan specimens from the North African Pleistocene fossils. Looking at the permutation test results (Table 5) confirms these visual observations, as Nataruk and the early Holocene specimens from Kenya are the only groups which are not statistically different.

The last bgPCA was run on the African populations only. Figure 6 presents the first two bgPCs, representing 61.84% of the variance. Along the first component (36.09% of the total variance) the general length of the mandible decreases from negative to positive values, the mandibular ramus becomes thinner and more elongated and the mentum osseum becomes more strongly developed along with the incurvatio mandibulae. The shape deformation associated with

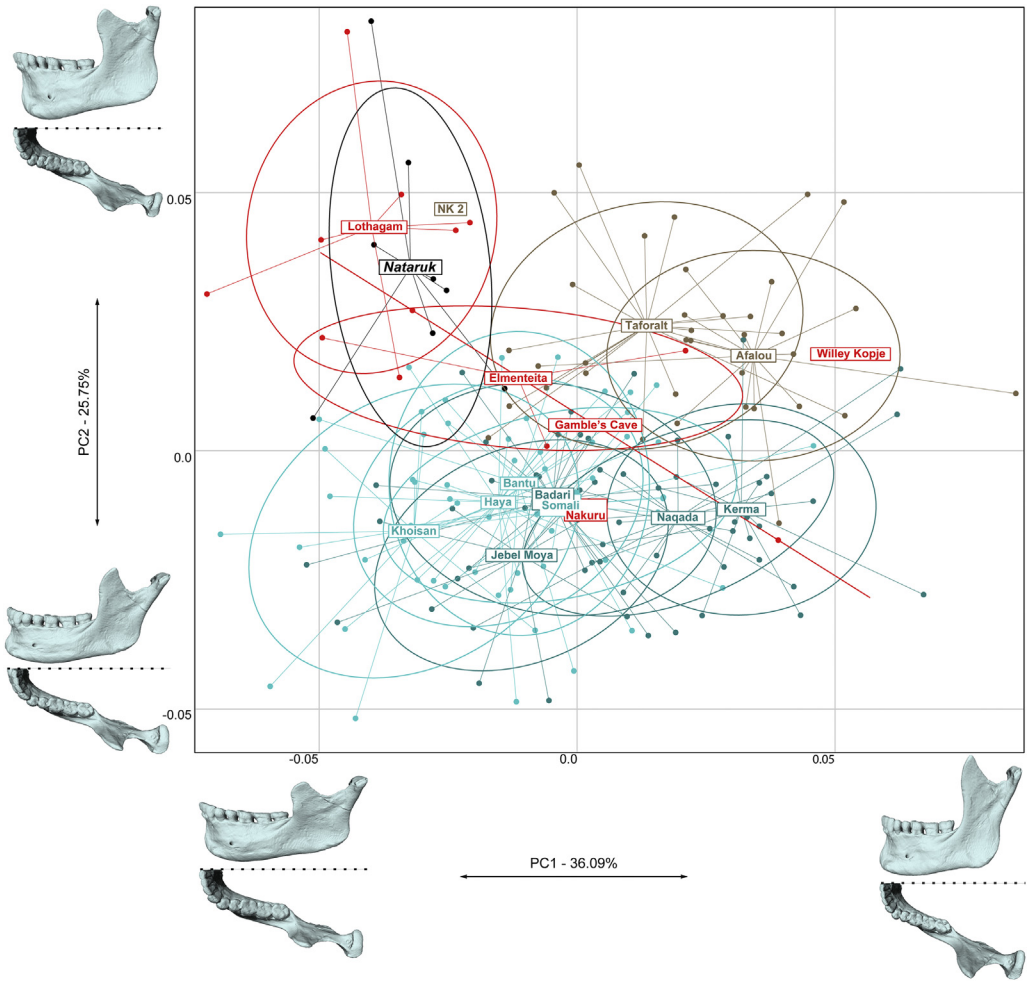

Figure 6. bgPCA showing the variation in shape within the mandibular sample grouped per African populations. The ellipses represent the 90% confidence interval for the estimated distribution of the specimens of each population. Each specimen is linked to the centroid of its group of origin. The Nataruk specimens are closer in shape to the Lothagam (red) and Nazlet Khater 2 (i.e., NK2, brown) specimens. (For interpretation of the references to color in this figure legend, the reader is referred to the Web version of this article.)

bgPC2 (25.75% of the variance) in the positive values represents a mandible with a deep mandibular body, the margins of which are strongly converging backwards, and a vertical ramus; on the negative side of the axis, the mandibular corpus is low with almost parallel margins, and the ramus is narrow, making a wide open angle with the corpus.

The morphospace (Fig. 6) separates on bgPC2, extant and pre-Dynastic Nile Valley populations from the Pleistocene and early Holocene ones, with the notable exception of Nakuru IX and one of the Gamble's Cave mandibles, which are positioned within the point clouds of recent Africans. On bgPC1, the sub-Saharan populations are separated from the Naqada and Kerma pre-Dynastic groups, while Badari and Jebel Moya appear to be more similar to the Somali, Bantu and Haya specimens. Regarding the Nataruk fossils, once again they are very similar to the mandibles from Lothagam, and to some of the Central Rift Valley fossils from Elmenteita and Gamble's Cave. It is worth noting that the shape of Willey Kopje II is closer to the North-African Pleistocene populations from Afalou and Taforalt than to the other early Holocene East African mandibles. The pairwise comparison of the group differences (Table 6) indicates first that groups with a low number of individuals (i.e., Gamble's Cave, Elmenteita, Nakuru, Willey Kopje and Nazlet Khater) cannot be assessed accurately, as they tend to show no significant differences to any of the other populations. Second, that the other populations can be generally distinguished, although the sub-Saharan groups are similar to each other, with the exception of the Khoisan. Finally, that the Nataruk mandibles are once again indistinguishable from those from Lothagam.

3.4. Phenetic affinities of the Nataruk specimens — phenograms

Finally, to assess the phenotypic affinity of the Nataruk specimens, we analyzed the mean shape of each population through PCAs and Neighbor-Joining trees based on the Euclidian distances with a 10,000 replication bootstrap. We performed this analysis separately on the 23 worldwide populations (Fig. 7A), the 10 meta-populations (Fig. 7B) and on the African populations only (Fig. 7C).

Figure 7A depicts the pattern of affinity between the 23 worldwide populations. On the left, the plot of the first two PCs from the PCA (56.23% of the variance) clearly shows the relatively unusual shape of the mandibles from Nataruk and Lothagam, which are similar only to the Pleistocene North-African Nazlet Khater 2 specimen. Most sub-Saharan African populations tend to cluster around the centre of the chart, while some Nile Valley groups and Eurasians occupy the lower left part of the morphospace. It is worth noting the apparent affinity in mandibular shape between the

Table 4
Between groups PCA – worldwide sample. *p*-values of pairwise group differences – based on permutation testing.

	Kerma	Jebel Moya	Naqada	Badari	Haya	Somali	Khoisan	Bantu	China	Sri Lanka	Andaman	Nicobar	Papua	Australia	Europe	Inuit	Holocene Central Rift	Lothagam	Pleistocene Europe	Afalou	Taforalt	Nazlet Khater 2
Jebel Moya	0.0004																					
Naqada	**0.2664**	0.0065																				
Badari	0.0004	**0.1373**	**0.1886**																			
Haya	0.0001	0.0125	0.0002	0.0718																		
Somali	0.0002	0.0376	0.0192	**0.1417**	0.0016																	
Khoisan	0.0001	**0.0913**	0.0001	0.0172	0.0340	0.0017																
Bantu	0.0012	**0.2409**	0.0315	**0.2023**	**0.7179**	**0.0856**	**0.1197**															
China	0.0004	**0.0516**	0.0058	0.0040	0.0012	0.0003	0.0050	0.0365														
Sri Lanka	0.0004	0.0007	0.0056	0.0009	0.0001	0.0001	0.0002	0.0044	0.0886													
Andaman	0.0001	0.0166	0.0003	0.0049	0.0286	0.0003	0.0214	**0.1457**	**0.1585**	**0.2219**												
Nicobar	0.0001	0.0135	0.0002	0.0029	0.0184	0.0001	0.0140	**0.1097**	**0.2199**	0.0326	**0.7160**											
Papua	0.0001	0.0014	0.0033	0.0001	0.0001	0.0001	0.0001	0.0040	**0.0554**	0.0365	0.0320	0.0017										
Australia	0.0223	0.0001	**0.1790**	0.0003	0.0001	0.0002	0.0001	0.0010	0.0002	0.0001	0.0001	0.0001	0.0034									
Europe	0.0001	0.0218	0.0001	0.0225	0.0007	0.0087	**0.0761**	0.0245	0.0005	0.0001	0.0001	0.0001	0.0001	0.0001								
Inuit	0.0286	0.0321	**0.2117**	0.0247	0.0001	0.0042	0.0001	0.0486	0.0278	0.0062	0.0046	0.0055	**0.0850**	**0.4329**	0.0001							
Holocene Central Rift	0.0131	0.0112	**0.1004**	**0.0805**	0.0087	**0.1086**	0.0066	**0.2595**	0.0012	0.0001	0.0012	0.0006	0.0008	0.0267	0.0104	0.0339						
Lothagam	0.0001	0.0001	0.0001	0.0001	0.0001	0.0001	0.0001	0.0002	0.0001	0.0001	0.0001	0.0001	0.0001	0.0001	0.0001	0.0001	0.0004					
Pleistocene Europe	0.0001	0.0053	0.0002	0.0068	0.0001	0.0016	0.0218	0.0107	0.0001	0.0001	0.0007	0.0008	0.0001	0.0001	0.0187	0.0004	0.0064	0.0001				
Afalou	0.0012	0.0001	0.0012	0.0001	0.0001	0.0001	0.0001	0.0001	0.0001	0.0001	0.0001	0.0001	0.0001	0.0001	0.0001	0.0001	0.0157	0.0001	0.0001			
Taforalt	0.0001	0.0001	0.0007	0.0004	0.0001	0.0001	0.0001	0.0010	0.0001	0.0001	0.0001	0.0001	0.0001	0.0001	0.0001	0.0001	0.0333	0.0001	0.0001	0.0018		
Nazlet Khater 2	**0.0825**	**0.1341**	**0.0850**	**0.2392**	**0.1264**	**0.2187**	**0.1915**	**0.2894**	0.0422	0.0444	**0.0709**	**0.0701**	0.0237	**0.0577**	**0.2407**	**0.0747**	**0.4750**	**0.7183**	**0.3679**	**0.0911**	**0.4273**	
Nataruk	0.0001	0.0001	0.0001	0.0001	0.0001	0.0001	0.0002	0.0028	0.0001	0.0001	0.0001	0.0001	0.0001	0.0001	0.0001	0.0001	**0.0109**	**0.1527**	0.0001	0.0001	0.0003	**0.8049**

Bold types: *p*-values > 0.05, indicating that the pairwise group difference is not significant.

Inuits and some sub-Saharan populations (Haya and Bantu) and with the Pleistocene European fossils. The late Pleistocene North African fossils from Afalou and Taforalt occupy a central bottom position in the morphospace, along with the early Holocene Central Rift specimens, the shapes of which are, nevertheless, less extreme. On the right, the unrooted phenogram appears divided into two main clusters. The upper part of the tree contains recent human populations, with the exception of the samples from Badari and Jebel Moya, and of Pleistocene European fossils, which cluster loosely with the Khoisan (18% of 10,000 bootstrap replications) and the Inuits (9%). sub-Saharan (Somali, Bantu and Haya) and Nile Valley (Badari and Jebel Moya) populations cluster on both sides of this group. The rest of this cluster is composed of South-East Asian and Oceanian populations, with a strong association of Australians and Andamans (42%) on the one hand, and of Papuans and Nicobarese (36%) on the other. The second main cluster is composed mainly of early Holocene or Pleistocene African specimens, as well as extant Eurasian mandibles. The North African samples from Afalou and Taforalt cluster together (43%), before grouping with a cluster that includes, sequentially, two Nile Valley populations, Naqada (27%) and Kerma (26%), and China and Europe (33%), which are closely associated (62%). Finally, the rest of the cluster is composed of the early Holocene Kenyan populations (Lothagam and Holocene Central Rift) and the North African Pleistocene mandible from Nazlet Khater, which are grouped around the Nataruk fossils. Nataruk is strongly associated with Nazlet Khater 2 (62%) and Lothagam (26%).

Figure 7B, which depicts the results based on the 10 meta-populations, shows a clearer phenetic signal. The morphospace defined by the first two PCs (67.85% of the variance) is divided between groups with PC1 values ≥ 0 and PC2 values ≤ 0 (Pleistocene North Africa, Holocene Kenya and Nataruk) and the opposite (all extant worldwide populations, as well as, again, the Pleistocene Europeans). Oceania, Asia and Europe tend to show an extreme of mandibular variation along PC1 (left of the morphospace), while extant sub-Saharan African, Inuit and, to a lesser extent, Nile Valley and Pleistocene European samples occupy a more central position. Pleistocene Europe and Pleistocene North Africa occupy opposite extremes along PC2. The unrooted tree on the right highlights a coherent phenetic pattern. The upper part of the tree shows the relationships between extant populations, with the sub-Saharan meta-population clustering (19%) with a group formed by Oceania and Asia (29%) and Europe and the North African Nile Valley (5%); the Inuit cluster with the Pleistocene Europeans (40%). The lower part of the phenogram is composed of the Pleistocene North Africans grouped with Nataruk (44%) and the other early Holocene East Africans (65%).

Finally, the last analysis concerns the African populations only, and allows us to compare Nataruk to individual sites from the Holocene Central Rift Valley of Kenya (Gamble's Cave and Elmenteita and the Neolithic sites of Willey Kopje and Nakuru). The morphospace depicted on Figure 7C represents 56.48% of the variance and indicates that recent African populations, along with Jebel Moya and the pre-Dynastic Badari, share a common morphospace in the bottom center of the chart. The other populations are more dispersed, and the oldest specimens tend to occupy the top of the morphospace. It is worth noting that Nakuru IX shows an extreme morphology which is nevertheless persistently closer to the Maghrebian fossils from Afalou and Taforalt than to any other sample or individual in the dataset, while Nataruk, Lothagam and Nazlet Khater share a common shape pattern. The unrooted phenogram (Fig. 7C, right) has two main branches. The first one is composed of recent sub-Saharan Africans (40%) grouped together with the prehistoric population from Sudan, Jebel Moya, and the pre-Dynastic Egyptians from Badari (22%), with two strongly

Table 5
Between groups PCA – worldwide meta-populations. *p*-values of pairwise group differences – based on permutation testing.

	Nile Valley	Sub-Sahara	Asia	Oceania	Europe	Inuit	Holocene Kenya	Pleistocene Europe	Pleistocene North Africa
Sub-Sahara	0.0001								
Asia	0.0001	0.0001							
Oceania	0.0001	0.0001	0.0004						
Europe	0.0001	0.0001	0.0003	0.0001					
Inuit	0.0001	0.0047	0.0001	0.0001	0.0001				
Holocene Kenya	0.0001	0.0001	0.0001	0.0001	0.0001	0.0001			
Pleistocene Europe	0.0001	0.0003	0.0001	0.0003	0.0001	0.0188	0.0001		
Pleistocene North Africa	0.0001	0.0001	0.0001	0.0001	0.0001	0.0001	0.0001	0.0001	
Nataruk	0.0001	0.0001	0.0001	0.0001	0.0001	0.0001	**0.2109**	0.0001	0.0001

Bold types: *p*-values > 0.05, indicating that the pairwise group difference is not significant.

supported clusters: Bantu-Haya (69%) and Khoisan-Jebel Moya (48%). The second branch supports two groups: a mostly Northern African one, with two Nile Valley populations (Naqada and Kerma, 48%) and the late Pleistocene fossils from Taforalt and Afalou (28%), and which includes the East African Nakuru IX specimen (48%); and a mostly East African one, which clusters all the other Central Rift Valley fossils (with a branch linking the fossils from Gamble's Cave and Willey Kopje II, 44%), along with a branch that includes the Elmenteita samples (45%) and a sub-cluster that groups the Nataruk-Lothagam mandibles (30%), with the Egyptian fossil from Nazlet Khater (64%).

In sum, while not all the resulting population clusters follow coherent affinity patterns, we note that some groupings reflect aspects of population history: the populations from Oceania with South Asians (Sri Lanka, Nicobar Is. and Andaman Is.), a mainland Eurasian grouping of Chinese and European populations, and most of the sub-Saharan groups which cluster tightly together. Additionally, the analyses highlight the diversity among the prehistoric Nile Valley populations, with two (Naqada and Kerma) recurrently associated with the late Pleistocene specimens from Afalou and Taforalt, as well as with the early Holocene Central Rift fossils, and the other two (Badari and Jebel Moya) more similar to extant sub-Saharan populations. Considering the phenotypic affinity of the Nataruk sample within both a worldwide and an African context, the analyses highlight the strong affinities that exist between Nataruk and other early Holocene populations from East Africa (i.e., Lothagam, Gamble's Cave and Elmenteita). They also show strong relationships with Pleistocene specimens from North Africa, Afalou and Taforalt and, more surprisingly, with the much older Nazlet Khater 2 specimen. These results place Nataruk within an East African, fisher-hunter-gatherer morphological continuum in the early Holocene, which shares strong affinities with late Pleistocene fossils from Northern Africa.

4. Discussion

This study of the mandibles from the site of Nataruk brings new information on the morphological variation of early Holocene populations from Eastern Africa. While previous studies have stressed the role of diet in shaping mandibular morphology (Lieberman, 2008; von Cramon-Taubadel, 2009b), recent evidence has weakened this interpretation (Katz et al., 2017). Both von Cramon-Taubadel (2009b) and Katz et al. (2017) conclude that the shape of the mandible does reflect subsistence strategy. However, von Cramon-Taubadel (2009b) suggests that this effect is very significant, to the extent that it erases the signature of past populations' history. Katz et al. (2017) have shown that mandibular phenotypic variation is mostly due to individual variation, which, when examined at a population level, shows that the impact of diet is dwarfed by neutral evolutionary processes. Results from the present study tend to support the second hypothesis, as without considering any environmental factors in the phenetic analyses of our mandibular sample, our results provide a clear recurrent phenetic and/or population history signal.

For instance, when looking at the size of the mandible of different populations, we note that populations representing different environments and dietary adaptations, such as Australians and Inuit (hunter-gatherers), and Europeans and Papuans (farmers/horticulturalists), cannot be distinguished in terms of centroid size (Fig. 3A). In fact, between-group centroid size variation in our sample is surprisingly low when considering extant human populations (Fig. 3A and B), with the exception of the Andaman Islanders, a group of Negritos from Southeast Asia. The small mandibular size of the latter is part of their distinctive overall small body size, reflected in a mean adult stature for males of ca. 148 cm (Stock and Migliano, 2009). Only the early Holocene and late Pleistocene fossils tend to be larger, and, in that respect, the Nataruk sample centroid size is within the expected variation from an early Holocene fisher-gatherer population from East Africa (Fig. 3).

In terms of the shape of the mandible of extant human populations, subsistence strategy does not seem to have a major impact on the results obtained. For instance, the results from the first bgPCA (Fig. 4) show that some of the hunter-gatherer groups (Australians and Andamanese) are not particularly separated from farmer/horticulturalist populations: the Andamanese are similar to the geographically close specimens from the Nicobar Islands, and Australians share similarities with the Nile Valley populations from the sites of Naqada and Kerma. The Neighbor-Joining analysis (Fig. 7A) shows a somewhat more ambiguous signal, as we note the clustering of the Australians with the Andamanese along with the clustering of Papuans with Nicobar Islanders. This pattern of similarities between hunter-gatherer on the one hand and farmer/horticulturalist on the other goes against genomic data which indicates a strong phylogenetic relationship between Australians and Papuans (Malaspinas et al., 2016). They, nevertheless, cluster into two closely related groups, which fall within a larger South-East Asia-Oceania cluster (i.e., Sri Lanka, Australia, Andaman, Papuan and Nicobar, see Fig. 7A). This association could depict the complex phenetic links between those populations that may reflect the differential retention of an ancient signature of dispersal (Lahr and Foley, 1994; Lahr, 1996; Reyes-Centeno et al., 2014; Pagani et al., 2016), the hypothesis of a deep genetic divergence of these groups from other South Asian populations (Bergström et al., 2016), and the shared pattern of archaic genomic admixture (Malaspinas et al., 2016; Mondal et al., 2016). The influence of population of origin in shaping the mandibular phenotype is also exemplified by some well-described phenetic patterns in the Neighbor-Joining trees (Fig. 7). For instance, in the worldwide population analysis, besides the clustering of the populations from Oceania and South Asia, the Chinese and Europeans are closely associated, a result that is also coherent with recent genomic studies (Mallick et al., 2016; Pagani et al., 2016).

Table 6
Between groups PCA – African sample. P-values of pairwise group differences – based on permutation testing.

	Kerma	Jebel Moya	Naqada	Badari	Haya	Somali	Khoisan	Bantu	Elmenteita	Gamble's Cave	Nakuru IX	Willey Kopje II	Lothagam	Afalou	Taforalt	Nazlet Khater2
Jebel Moya	0.0003															
Naqada	**0.2394**	0.0055														
Badari	0.0002	**0.1232**	**0.1681**													
Haya	0.0001	0.0098	0.0002	**0.0628**												
Somali	0.0001	0.0295	0.0123	**0.1222**	0.0007											
Khoisan	0.0001	**0.0742**	0.0001	0.0122	0.0244	0.0013										
Bantu	0.0008	**0.2243**	0.0231	**0.1797**	**0.7014**	**0.0728**	**0.0989**									
Elmenteita	0.0461	**0.1469**	**0.1126**	**0.3342**	**0.224**	**0.2158**	**0.2048**	**0.7015**								
Gamble's Cave	**0.4104**	**0.376**	**0.4918**	**0.4786**	**0.27**	**0.6254**	**0.1646**	**0.5741**	**0.8565**							
Nakuru IX	**0.4712**	**0.5815**	**0.7551**	**0.7403**	**0.4483**	**0.8738**	**0.6092**	**0.6378**	**0.6567**	**0.9586**						
Willey Kopje II	**0.2919**	**0.0579**	**0.4176**	**0.1324**	**0.0933**	**0.1408**	0.0396	**0.1508**	**0.2964**	**0.4919**	**0.6525**					
Lothagam	0.0001	0.0001	0.0001	0.0001	0.0001	0.0001	0.0001	0.0001	**0.1096**	**0.0664**	**0.0721**	0.0202				
Afalou	0.0011	0.0001	0.0006	0.0001	0.0001	0.0001	0.0001	0.0001	0.038	**0.2655**	**0.2821**	**0.8223**	0.0001			
Taforalt	0.0001	0.0001	0.0005	0.0001	0.0001	0.0001	0.0001	0.0003	**0.1702**	**0.261**	**0.4905**	**0.3508**	0.0001	0.0016		
Nazlet Khater 2	**0.0887**	**0.1322**	**0.0936**	**0.2121**	**0.1275**	**0.2013**	**0.1767**	**0.2625**	**0.8323**	**0.5047**	**0.4527**	**0.1171**	**0.6793**	**0.0972**	**0.3867**	
Nataruk	0.0001	0.0001	0.0001	0.0001	0.0001	0.0001	0.0002	0.0012	**0.3296**	**0.189**	**0.3547**	0.0398	**0.1302**	0.0001	0.0001	**0.7613**

Bold types: p-values >0.05, indicating that the pairwise group difference is not significant.

The shape analyses also show that all the specimens older than 5000 years BP (i.e., early Holocene and Pleistocene) occupy the same sector of the morphospace defined by the first 2 PCs of the PCAs run on the mean shape of the different populations (Fig. 7), the only exception being the Pleistocene European sample, which tends to share affinities with the Inuit and recent Sub-Saharan (especially Khoisan) populations (Fig. 7A and B). Such an association between geographically and/or chronologically distant hunter-gatherer groups (Pleistocene Europe, Khoisan and Inuit), may nevertheless not be indicative of a functional response of mandibular morphology to their shared subsistence strategy, since morphological and ancient genomic results suggest that both the South African Khoisan and the Inuit may preserve signatures of complex ancestral relationships with Pleistocene Europeans (Grine et al., 2007; Raghavan et al., 2014; Flegontov et al., 2016; Schlebusch et al., 2017). Some of the prehistoric populations of the Nile Valley (Naqada and Kerma) show strong similarities with the late Pleistocene North African fossils from Afalou and Taforalt (Fig. 7A and C). This affinity seems to represent phylogenetic proximity, as those populations lived in different environments and did not share a common subsistence strategy: Afalou and Taforalt were hunter-gatherers (Aoudia-Chouakri, 2013) while Naqada and Kerma were early farmers (Simon, 1989; Hendrickx, 1999). However, the other Nile Valley populations cluster differently: Jebel Moya and Badari show similarities with sub-Saharan African samples (Khoisan, Somali, Haya and Bantu). This latter pattern is recurrent, and may be partly explained by the complexity of the site of Jebel Moya. The site, which includes three occupation phases (Gerharz, 1994; Brass and Schwenniger, 2013), lies at the boundary between North and sub-Saharan African geographic spheres (Brass, 2014) and may preserve an admixed population exhibiting a mosaic of features that are reminiscent of both sub-Saharan and North African peoples (Irish and Konigsberg, 2007). The sub-Saharan affinities of the early pre-Dynastic population from the Egyptian site of Badari observed recurrently in our analyses should be investigated further. The best evidence that mandibular morphology captures phenetic relations is the close association between the Nataruk and Lothagam mandibles observed in every analysis performed. These two samples originate from sites that are spatially and temporally close, and probably represent sub-groups from a single population of fisher-foragers of Southwest Turkana during the early phase of the African Humid Period. Mandibular morphology captures the underlying phenetic signal that describes this close relationship.

As a whole, our morphometric data provide a phenotypic signal that can be interpreted clearly in a phenetic framework.

4.1. Who were the Nataruk people? – Phenetic affinity of the mandibles from Nataruk

The results from this study recurrently show that the Nataruk mandibles share their strongest affinities with the Lothagam specimens as hypothesised: they are similar in size (Fig. 3A and C) and similar in shape, as illustrated by both the bgPCAs results (Figs. 3, 4 and 5) and by their mean Procrustes distance and position in the Neighbor-Joining trees (Fig. 7A and C). This affinity is expected, since the two sites are in close geographical proximity (about 25 km apart) and of overall similar age (Robbins, 1974; Mirazón Lahr et al., 2016), and could represent sub-groups from the same population. The second expectation, that the Nataruk mandibles would share shape affinities with early Holocene specimens from East Africa, here represented by a sample from the Central Rift Valley, is also met, as exemplified by the clustering of most of the Central Rift specimens with Nataruk in all three Neighbor-Joining trees (Fig. 7). Those affinities are supported by strong bootstrap values which underline the likely phylogenetic

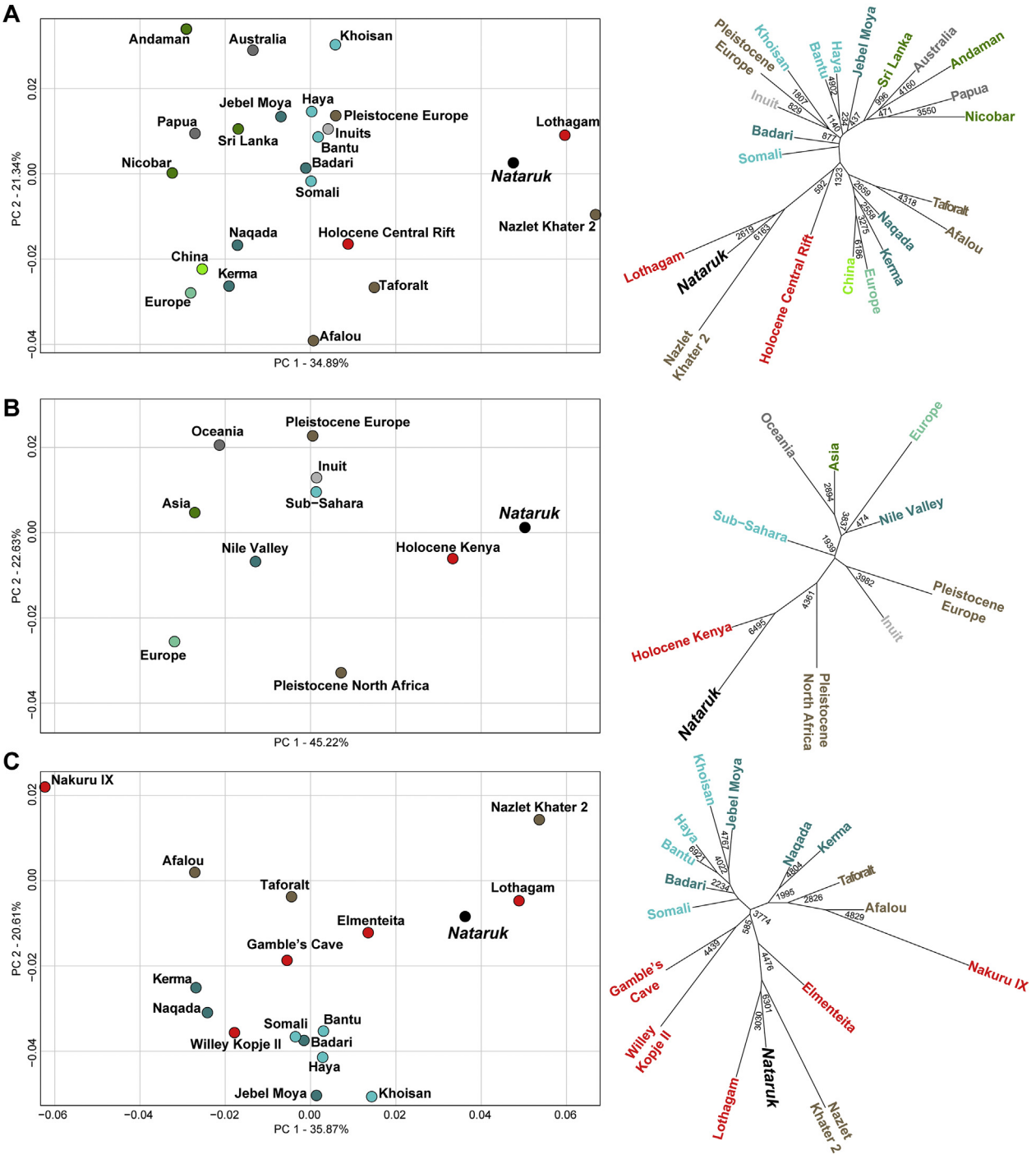

Figure 7. PCAs run on the mean shape of each population and associated unrooted Neighbor-Joining trees with a 10,000 replications bootstrap. (A) worldwide populations, (B) worldwide meta-populations, and (C) African populations. In each tree, the Nataruk and Lothagam specimens (Holocene Kenya in 7 B) cluster together.

links between Eastern African populations dated between 10,000 and 6000 thousands years BP. Nakuru IX is the only one of the Holocene Central Rift Valley specimens not to cluster around the Nataruk sample. This morphological difference may be explained by different factors. First, being a single specimen, we are aware that its morphology may not adequately reflect the phenotype of its population of origin, and that the Nakuru IX mandible may represent an extreme of the morphological variation of its people. Second, the site of Nakuru is younger (Neolithic) than most of the early Holocene sample of the study; however, another Neolithic specimen from the same area, Willey Kopje II, does cluster around Nataruk along with the other Holocene Central Rift Valley specimens (Fig. 7C), suggesting that age and subsistence is not what pulls the fossil of Nakuru IX apart from other Holocene East Africans. Instead, Nakuru IX persistently shares strong affinities with the North African late Pleistocene fossils from Taforalt and Afalou (15,000 to 11,000 years BP), which, as observed in the worldwide analysis, also cluster with the Nile Valley North African fossils from Naqada and Kerma. Similarly, the much older (36,000 years BP) Nile Valley fossil from Nazlet Khater clusters with the early Holocene Eastern African specimens, suggesting an ancient connection between East Africa and the Nile Valley.

It is interesting to note that the third Neighbor-Joining tree including only African specimens (Fig. 7C) depicts clearly three different branches, each associated with a set of older populations – (1) extant sub-Sahara Africans, including the pre-Dynastic Badari, and the Nubian Jebel Moya; (2) early Holocene Eastern Africans (including Nataruk) and the fossil from Nazlet Khater 2; and (3) a similar diachronic and geographically dispersed association among late Pleistocene groups from the Maghreb (Afalou and Taforalt), the pre-Dynastic and Nubian samples from Naqada and Kerma from the Nile Valley, and the Neolithic fossil (Nakuru IX) from the Central Rift Valley of Kenya as observed above. The last two clusters seem to share more affinities between themselves than with the extant sub-Saharan Africans.

In sum, the Nataruk mandibles are part of a continuum of morphological variation that links Pleistocene and Holocene populations from Eastern and Northern Africa (Maghreb, Nile Valley and the Kenyan Rift Valley) to the almost complete exclusion of the recent African sample.

Such a pattern can be interpreted first through the global climatic change that impacted the world at the end of the Pleistocene. The last deglaciation, which started in the Northern Hemisphere around 19,000 years ago and in the Southern hemisphere around 15,000 years ago, led to two abrupt rises in sea level (Clark et al., 2009), leading to the onset of an interglacial period worldwide and, in the case of Africa, to a period of greatly increased precipitation known as the African Humid Period (de Menocal et al., 2000). In this framework, the greening of the Sahara (Larrasoaña et al., 2013) may have allowed hunting–fishing populations to spread from the Northern Kenyan lakes to the Nile and across the Sahel into North Africa (Mirazón Lahr, 2016). The African Humid Period lasted until around 5000 years ago (de Menocal, 2015), presumably creating multiple opportunities of increased population connectivity between Eastern and Northern Africa for 10,000 years. It is of interest to note that most of the populations representing North Africa in our sample date to within this time span, when aquatic corridors would have allowed some connection and, presumably, gene-flow: the specimens from Afalou and Taforalt, which are dated between 15,000 and 11,000 years BP (Aoudia-Chouakri, 2013), and the specimens from Naqada, Badari and Jebel Moya, who lived in the Nile Valley from 6000 to 5000 years ago (Gerharz, 1994; Hendrickx, 1999). Only the Kerma specimens, dated to around 3500 years BP (Simon, 1989), and the Nazlet Khater 2 fossil dated to 36,000 years BP (Crevecoeur, 2006), are outside of the temporal span in which this North-East African connection would have existed, although they may reflect both lagged patterns of survivorship/affinity (Kerma) and biogeographically recurrent connections (Nazlet Khater).

Additionally, the site of Nataruk is located at the edge of a large paleolake (Turkana). The lithic assemblage that was uncovered at the site is similar to other Later Stone Age assemblages in that area (Robbins, 2006; Beyin, 2011), including fragments of barbed bone harpoons typical of early Holocene fisher-foragers of Turkana (Robbins, 1975). As a result, the Nataruk people have been described as representing a hunter-fisher-gatherer population (Mirazón Lahr et al., 2016). Within the comparative sample of the present study, other populations present similar characteristics in terms of chronology and lifestyle: the Lothagam sample, which originates from a site that is also situated at the edge of Lake Turkana and is dated to a similar period (Robbins, 1974), and the Central Rift Valley specimens that originate from populations that lived in the Nakuru-Elmenteita Basin between 8000 and 6000 years BP. Although Nakuru and Elmenteita are two different lakes nowadays, they formed a much larger paleolake during the early Holocene (Dühnforth et al., 2006), which may have also supported a fisher-forager subsistence strategy during the African Humid Period, consistent with the presence of a bone harpoon at the site of Gamble's Cave (Oakley, 1961). Although more complete information concerning the life-style of the hunter-gatherers who lived in the other sites of the area at the time, such as Elmenteita (Leakey, 1970), is wanting, the geographic, ecological and chronostratigraphic position of the populations living at the edge of the Nakuru-Elmenteita paleolake in the early Holocene suggest that they may have experienced similar conditions and may have shown similar adaptive responses to the Nataruk-Lothagam population, as well as possibly shared ancestry. Lastly, the Afalou and Taforalt North African groups lived near the Mediterranean coast and have also been described as hunter-fisher-gatherers (Aoudia-Chouakri, 2013); their relationship to AHP Saharan and Nile Valley populations remains to be fully explored.

Finally, it is interesting to note that neither the late Pleistocene North African sample, nor the early Holocene Eastern African specimens, including the Nataruk fossils, show strong affinities to the specimens representing the extant African populations in our sample. As it has been pointed out in the morphological description of other late Pleistocene/early Holocene African fossils (Harvati et al., 2011; Tryon et al., 2015; Crevecoeur et al., 2016), these specimens tend to exhibit distinctive characteristics and higher phenotypic diversity than do extant African populations, to the extent that they show more affinities with Middle to early late Pleistocene fossils (Crevecoeur et al., 2016). Such a phenotypic pattern may explain the affinity shared by the Nataruk fossils and the late Pleistocene fossil from Nazlet Khater 2 in our analyses, and highlights the role of an early Holocene Filter in shaping current patterns of human diversity, particularly in Africa (Mirazón Lahr, 2016).

5. Conclusion

This study attempts to establish the phenetic affinities of the people of Nataruk, a hunter-fisher-gatherer population from the early Holocene of West Turkana (Kenya), on the basis of their mandibular morphology. Our findings resonate with previously observed patterns of phenotypic plasticity in the human mandible, the morphology of which reflects, in part, recent adaptations to environmental and behavioral factors. However, the main signal in our analyses is one that appears to reflect population history. In the case of the people who were killed at Nataruk, we show their strong affinities with other early Holocene hunter-fisher-gatherer populations from West Turkana in particular, and Eastern Africa more generally, but also, and more surprisingly, the apparent phenetic connection that may have existed between these Eastern African populations and some Nile Valley and Maghrebian groups which lived at a time when a Green Sahara may have allowed substantial contact, and potential gene flow, across a vast expanse of Northern and Eastern Africa. It is possible that the shared aquatic fisher-forager strategies of populations who lived geographically separated by the Sahara could have led to a common adaptive response that is reflected in the shape of the mandible, thus convergently accounting for the strong affinities observed in the data. However, such overriding functional convergence is not supported by the results of the worldwide analyses that recurrently cluster groups of different subsistence strategy, nor with the totality of the observed phenotypic pattern among the early Holocene African samples. This is further stressed by the fact that this morphological association is not exclusive to AHP fisher-foragers, but also includes populations in both the Nile Valley and Kenyan Central Rift Valley who practised a pastoralist and/or agriculturalist subsistence strategy around the end of the African Humid Period. Given the limited number of late Pleistocene/early Holocene African fossils available and the poor understanding of the archaeological context of some of the Central

Rift Valley specimens, further research is needed to bring additional insight into the history of early African populations.

Acknowledgements

This study was funded by an Advanced ERC Award (IN-AFRICA Project, grant number: 295907). For permission to carry out field and museum research in Kenya, we thank the Office of the President of Kenya, the Turkana County government, the National Museums of Kenya, and the people of Turkana. For permission to study specimens in their care, we thank directors and curators of the following institutions: Musée de l'Homme (Paris, France); Institut de Paléontologie Humaine (Paris, France); National Museums of Kenya (Nairobi, Kenya); Anthropos Institute (Brno, Czech Republic), Open Scan Research Archive (University of Pennsylvania Museum of Archaeology and Anthropology, USA), and Duckworth Laboratory (Cambridge, UK). We thank F. Lahr for assistance with CT-scanning, Isabelle Crevecoeur, Patrick Semal and Stéphane Louryan for providing access to the CT-scan of Nazlet Khater 2, and Todd Rae, Janet Monge and Thomas Schoenemann for helping with the ORSA database. We thank F. Détroit, M. Galland and J. Corny for help and ideas. Finally, we thank M. Plavcan, the Associate Editor, and two anonymous reviewers for valuable comments and criticisms of earlier drafts that contributed to the improvement of this study.

Supplementary Online Material

Supplementary online material related to this article can be found at https://doi.org/10.1016/j.jhevol.2018.04.013.

References

Adams, D.C., Otárola-Castillo, E., 2013. Geomorph: an R package for the collection and analysis of geometric morphometric shape data. Methods in Ecology and Evolution 4, 393–399.
Aoudia-Chouakri, L., 2013. Pratiques funéraires complexes: réévaluation archéo-anthropologique des contextes Ibéromaurusiens et Capsiens (paléolithique supérieur et épipaléolithique, Afrique du nord-ouest). Ph.D. Dissertation, Université de Bordeaux 1.
Bergström, A., Nagle, N., Chen, Y., McCarthy, S., Pollard, M.O., Ayub, Q., Wilcox, S., Wilcox, L., van Oorschot, R.A.H., McAllister, P., Williams, L., Xue, Y., Mitchell, R.J., Tyler-Smith, C., 2016. Deep roots for Aboriginal Australian Y chromosomes. Current Biology 25, 809–813.
Betti, L., Balloux, F., Hanihara, T., Manica, A., 2010. The relative role of drift and selection in shaping the human skull. American Journal of Physical Anthropology 141, 76–82.
Beyin, A., 2011. Recent archaeological survey and excavation around the Greater Kalokol Area, west side of Lake Turkana: Preliminary findings. Nyame Akuma 75, 40–50.
Bookstein, F.L., 1989. Principal warps: thin-plate splines and the decomposition of deformations. IEEE TPAMI 11, 567–585.
Brass, M., 2014. The southern frontier of the Meroitic state: The view from Jebel Moya. African Archaeological Review 31, 425–445.
Brass, M., Schwenniger, J.-L., 2013. Jebel Moya (Sudan): new dates from a mortuary complex at the southern Meroitic frontier. Azania 48, 455–472.
Bricker, H., Mellars, P., 1987. Datations 14C de l'Abri Pataud (Les Eyzies, Dordogne) par le procédé "accélérateur-spectromètre de masse. L'Anthropologie 91, 227–234.
Buikstra, J.E., Ubelaker, D.H., 1994. Standards for data collection from human skeletal remains. Arkansas Archeological Survey, Fayetteville, AK.
Carolin, S.A., Cobb, K.M., Adkins, J.F., Clark, B., Conroy, J.L., Lejau, S., Malang, J., Tuen, A.A., 2013. Varied response of western Pacific hydrology to climate forcings over the last glacial period. Science 340, 1564–1566.
Clark, P.U., Dyke, A.S., Shakun, J.D., Carlson, A.E., Clark, J., Wohlfarth, B., Mitrovica, J.X., Hostetler, S.W., McCabe, A.M., 2009. The Last Glacial Maximum. Science 325, 710–714.
Collett, M., 1933. A study of twelfth and thirteenth dynasty skulls from Kerma (Nubia). Biometrika 25, 254–284.
Creed-Miles, M., Rosas, A., Kruszynski, R., 1996. Issues in the identification of Neandertal derivative traits at early post-natal stages. Journal of Human Evolution 30, 147–153.
Crevecoeur, I., 2006. Etude anthropologique des restes humains de Nazlet Khater (Paléolithique supérieur, Egypte). Ph.D. Dissertation, Université de Bordeaux 1.
Crevecoeur, I., Brooks, A., Ribot, I., Cornelissen, E., Semal, P., 2016. Late Stone Age human remains from Ishango (Democratic Republic of Congo): New insights on Late Pleistocene modern human diversity in Africa. Journal of Human Evolution 96, 35–57.
Daegling, D., 2010. Understanding Skull Function from a Mechanobiological Perspective. In: Larsen, C.S. (Ed.), A Companion to Biological Anthropology. Blackwell Publishing Ltd, Oxford, UK, pp. 501–515.
Day, M., 1969. Omo human skeletal remains. Nature 222, 1135–1138.
de Menocal, P.B., 2015. Palaeoclimate: End of the African Humid Period. Nature Geoscience 8, 86–87.
de Menocal, P., Ortiz, J., Guilderson, T., Adkins, J., Sarnthein, M., Baker, L., Yarusinsky, M., 2000. Abrupt onset and termination of the African Humid Period: rapid climate responses to gradual insolation forcing. Quaternary Science Reviews 19, 347–361.
Dray, S., Dufour, A.-B., 2007. The ade4 Package: Implementing the Duality Diagram for Ecologists. Journal of Statistical Software 22, 20.
Dühnforth, M., Bergner, A.G.N., Trauth, M.H., 2006. Early Holocene water budget of the Nakuru-Elmenteita basin, Central Kenya Rift. Journal of Paleolimnology 36, 281–294.
Dutour, O., 1989. Hommes Fossiles du Sahara. Peuplements holocènes du Mali septentrional. Editions du CNRS, Paris.
Fleagle, J.G., Assefa, Z., Brown, F.H., Shea, J.J., 2008. Paleoanthropology of the Kibish Formation, southern Ethiopia: Introduction. Journal of Human Evolution 55, 360–365.
Flegontov, P., Changmai, P., Zidkova, A., Logacheva, M.D., Altınışık, N.E., Flegontova, O., Gelfand, M.S., Gerasimov, E.S., Khrameeva, E.E., Konovalova, O.P., Neretina, T., Nikolsky, Y.V., Starostin, G., Stepanova, V.V., Travinsky, I.V., Tříska, M., Tříska, P., Tatarinova, T.V., 2016. Genomic study of the Ket: a Paleo-Eskimo-related ethnic group with significant ancient North Eurasian ancestry. Scientific Reports 6, 20768.
Galland, M., 2013. Le premier peuplement des Amériques: application de la morphométrie géométrique 3D à la variation crânienne actuelle et fossile. Ph.D. Dissertation, Muséum national d'Histoire naturelle.
Gasse, F., 2000. Hydrological changes in the African tropics since the Last Glacial Maximum. Quaternary Science Reviews 19, 189–211.
Gerharz, R., 1994. Jebel Moya. Akademie Verlag, Berlin.
González-José, R., Ramírez-Rozzi, F., Sardi, M., Martínez-Abadías, N., Hernández, M., Pucciarelli, H.M., 2005. Functional-cranial approach to the influence of economic strategy on skull morphology. American Journal of Physical Anthropology 128, 757–771.
Gower, J.C., 1975. Generalised Procrustes analysis. Psychometrika 40, 33–50.
Grine, F.E., 2016. The Late Quaternary hominins of Africa: The skeletal evidence from MIS 6-2. In: Jones, S.C., Stewart, B.A. (Eds.), Africa from MIS 6-2. Population Dynamics and Paleoenvironments. Springer, Dordrecht, pp. 323–381.
Grine, F.E., Bailey, R.M., Harvati, K., Nathan, R.P., Morris, A.G., Henderson, G.M., Ribot, I., Pike, A.W.G., 2007. Late Pleistocene human skull from Hofmeyr, South Africa, and modern human origins. Science 315, 226–229.
Harvati, K., Weaver, T.D., 2006. Human cranial anatomy and the differential preservation of population history and climate signatures. Anatomical Record 288A, 1225–1233.
Harvati, K., Stringer, C., Grün, R., Aubert, M., Allsworth-Jones, P., Folorunso, C.A., 2011. The Later Stone Age calvaria from Iwo Eleru, Nigeria: Morphology and chronology. PLoS ONE 6, e24024.
Hendrickx, S., 1999. La chronologie de la préhistoire tardive et des débuts de l'histoire de l'Egypte. Archéo-Nil 9, 13–81.
Hublin, J.-J., Ben-Ncer, A., Bailey, S.E., Freidline, S.E., Neubauer, S., Skinner, M.M., Bergmann, I., Le Cabec, A., Benazzi, S., Harvati, K., Gunz, P., 2017. New fossils from Jebel Irhoud, Morocco and the pan-African origin of *Homo sapiens*. Nature 546, 289–292.
Irish, J.D., Konigsberg, L., 2007. The ancient inhabitants of Jebel Moya redux: measures of population affinity based on dental morphology. International Journal of Osteoarchaeology 17, 138–156.
Katz, D.C., Grote, M.N., Weaver, T.D., 2017. Changes in human skull morphology across the agricultural transition are consistent with softer diets in preindustrial farming groups. Proceedings of the National Academy of Sciences USA 114, 9050–9055.
Lahr, M., 1996. The Evolution of Modern Human Diversity: A Study of Cranial Variation. Cambridge University Press, Cambridge.
Lahr, M.M., Foley, R.A., 1994. Multiple dispersals and modern human origins. Evolutionary Anthropology 3, 48–60.
Larrasoaña, J.C., Roberts, A.P., Rohling, E.J., 2013. Dynamics of green Sahara periods and their role in hominin evolution. PLoS ONE 8, e76514.
Leakey, L.S.B., 1970. The Stone Age Races of Kenya. Oxford University Press, London.
Leakey, R.E.F., 1969. Early *Homo sapiens* remains from the Omo River region of South-west Ethiopia: Faunal remains from the Omo Valley. Nature 222, 1132–1133.
Li, J.Z., Absher, D.M., Tang, H., Southwick, A.M., Casto, A.M., Ramachandran, S., Cann, H.M., Barsh, G.S., Feldman, M., Cavalli-Sforza, L.L., Myers, R.M., 2008. Worldwide human relationships inferred from genome-wide patterns of variation. Science 319, 1100–1104.
Lieberman, D.E., 2008. Speculations about the selective basis for modern human craniofacial form. Evolutionary Anthropology 17, 55–68.
Liu, H., Prugnolle, F., Manica, A., Balloux, F., 2006. A geographically explicit genetic model of worldwide human-settlement history. American Journal of Human Genetics 79, 230–237.
Malaspinas, A.-S., Westaway, M.C., Muller, C., Sousa, V.C., Lao, O., Alves, I., Bergström, A., Athanasiadis, G., Cheng, J.Y., Crawford, J.E., Heupink, T.H., Macholdt, E., Peischl, S., Rasmussen, S., Schiffels, S., Subramanian, S., Wright, J.L.,

Albrechtsen, A., Barbieri, C., Dupanloup, I., Eriksson, A., Margaryan, A., Moltke, I., Pugach, I., Korneliussen, T.S., Levkivskyi, I.P., Moreno-Mayar, J.V., Ni, S., Racimo, F., Sikora, M., Xue, Y., Aghakhanian, F.A., Brucato, N., Brunak, S., Campos, P.F., Clark, W., Ellingvåg, S., Fourmile, G., Gerbault, P., Injie, D., Koki, G., Leavesley, M., Logan, B., Lynch, A., Matisoo-Smith, E.A., McAllister, P.J., Mentzer, A.J., Metspalu, M., Migliano, A.B., Murgha, L., Phipps, M.E., Pomat, W., Reynolds, D., Ricaut, F.-X., Siba, P., Thomas, M.G., Wales, T., Wall, C.M.r, Oppenheimer, S.J., Tyler-Smith, C., Durbin, R., Dortch, J., Manica, A., Schierup, M.H., Foley, R.A., Lahr, M.M., Bowern, C., Wall, J.D., Mailund, T., Stoneking, M., Nielsen, R., Sandhu, M.S., Excoffier, L., Lambert, D.M., Willerslev, E., 2016. A genomic history of Aboriginal Australia. Nature 538, 207–214.

Mallick, S., Li, H., Lipson, M., Mathieson, I., Gymrek, M., Racimo, F., Zhao, M., Chennagiri, N., Nordenfelt, S., Tandon, A., Skoglund, P., Lazaridis, I., Sankararaman, S., Fu, Q., Rohland, N., Renaud, G., Erlich, Y., Willems, T., Gallo, C., Spence, J.P., Song, Y.S., Poletti, G., Balloux, F., van Driem, G., de Knijff, P., Romero, I.G., Jha, A.R., Behar, D.M., Bravi, C.M., Capelli, C., Hervig, T., Moreno-Estrada, A., Posukh, O.L., Balanovska, E., Balanovsky, O., Karachanak-Yankova, S., Sahakyan, H., Toncheva, D., Yepiskoposyan, L., Tyler-Smith, C., Xue, Y., Abdullah, M.S., Ruiz-Linares, A., Beall, C.M., Di Rienzo, A., Jeong, C., Starikovskaya, E.B., Metspalu, E., Parik, J., Villems, R., Henn, B.M., Hodoglugil, U., Mahley, R., Sajantila, A., Stamatoyannopoulos, G., Wee, J.T.S., Khusainova, R., Khusnutdinova, E., Litvinov, S., Ayodo, G., Comas, D., Hammer, M.F., Kivisild, T., Klitz, W., Winkler, C.A., Labuda, D., Bamshad, M., Jorde, L.B., Tishkoff, S.A., Watkins, W.S., Metspalu, M., Dryomov, S., Sukernik, R., Singh, L., Thangaraj, K., Pääbo, S., Kelso, J., Patterson, N., Reich, D., 2016. The Simons Genome Diversity Project: 300 genomes from 142 diverse populations. Nature 538, 201–206.

Marom, A., McCullagh, J.S., Higham, T.F., Sinitsyn, A.A., Hedges, R.E., 2012. Single amino acid radiocarbon dating of Upper Paleolithic modern humans. Proceedings of the National Academy of Sciences USA 109, 6878–6881.

Mirazón Lahr, M., 2016. The shaping of human diversity: filters, boundaries and transitions. Philosophical Transactions of the Royal Society B: Biological Sciences 371, 1698.

Mirazón Lahr, M., Foley, R.A., 2016. Human evolution in Late Quaternary Eastern Africa. In: Jones, S.C., Stewart, B.A. (Eds.), Africa From MIS 6-2. Population Dynamics and Paleoenvironments. Springer, Dordrecht, pp. 215–231.

Mirazón Lahr, M., Rivera, F., Power, R.K., Mounier, A., Copsey, B., Crivellaro, F., Edung, J.E., Fernandez, J.M.M., Kiarie, C., Lawrence, J., Leakey, A., Mbua, E., Miller, H., Muigai, A., Mukhongo, D.M., Van Baelen, A., Wood, R., Schwenninger, J.L., Grün, R., Achyuthan, H., Wilshaw, A., Foley, R.A., 2016. Inter-group violence among early Holocene hunter-gatherers of West Turkana, Kenya. Nature 529, 394–398.

Mondal, M., Casals, F., Xu, T., Dall'Olio, G.M., Pybus, M., Netea, M.G., Comas, D., Laayouni, H., Li, Q., Majumder, P.P., Bertranpetit, J., 2016. Genomic analysis of Andamanese provides insights into ancient human migration into Asia and adaptation. Nature Genetics 48, 1066–1070.

Mounier, A., Marchal, F., Condemi, S., 2009. Is *Homo heidelbergensis* a distinct species? New insight on the Mauer mandible. Journal of Human Evolution 56, 219–246.

Nicholson, E., Harvati, K., 2006. Quantitative analysis of human mandibular shape using three-dimensional geometric morphometrics. American Journal of Physical Anthropology 131, 368–383.

Noback, M.L., Harvati, K., 2015a. The contribution of subsistence to global human cranial variation. Journal of Human Evolution 80, 34–50.

Noback, M.L., Harvati, K., 2015b. Covariation in the human masticatory apparatus. Anatomical Record 298, 64–84.

Noback, M.L., Harvati, K., Spoor, F., 2011. Climate-related variation of the human nasal cavity. American Journal of Physical Anthropology 145, 599–614.

Oakley, K.P., 1961. Bone harpoon from Gamble's Cave, Kenya. The Antiquaries Journal 41, 86–87.

Pagani, L., Lawson, D.J., Jagoda, E., Mörseburg, A., Eriksson, A., Mitt, M., Clemente, F., Hudjashov, G., DeGiorgio, M., Saag, L., Wall, J.D., Cardona, A., Mägi, R., Sayres, M.A.W., Kaewert, S., Inchley, C., Scheib, C.L., Järve, M., Karmin, M., Jacobs, G.S., Antao, T., Iliescu, F.M., Kushniarevich, A., Ayub, Q., Tyler-Smith, C., Xue, Y., Yunusbayev, B., Tambets, K., Mallick, C.B., Saag, L., Pocheshkhova, E., Andriadze, G., Muller, C., Westaway, M.C., Lambert, D.M., Zoraqi, G., Turdikulova, S., Dalimova, D., Sabitov, Z., Sultana, G.N.N., Lachance, J., Tishkoff, S., Momynaliev, K., Isakova, J., Damba, L.D., Gubina, M., Nymadawa, P., Evseeva, I., Atramentova, L., Utevska, O., Ricaut, F.-X., Brucato, N., Sudoyo, H., Letellier, T., Cox, M.P., Barashkov, N.A., Škaro, V., Mulahasanović, L., Primorac, D., Sahakyan, H., Mormina, M., Eichstaedt, C.A., Lichman, D.V., Abdullah, S., Chaubey, G., Wee, J.T.S., Mihailov, E., Karunas, A., Litvinov, S., Khusainova, R., Ekomasova, N., Akhmetova, V., Khidiyatova, I., Marjanović, D., Yepiskoposyan, L., Behar, D.M., Balanovska, E., Metspalu, A., Derenko, M., Malyarchuk, B., Voevoda, M., Fedorova, S.A., Osipova, L.P., Lahr, M.M., Gerbault, P., Leavesley, M., Migliano, A.B., Petraglia, M., Balanovsky, O., Khusnutdinova, E.K., Metspalu, E., Thomas, M.G., Manica, A., Nielsen, R., Villems, R., Willerslev, E., Kivisild, T., Metspalu, M., 2016. Genomic analyses inform on migration events during the peopling of Eurasia. Nature 538, 238–241.

Protsch, R., 1978. The chronological position of Gamble's Cave II and Bromhead's Site (Elmenteita) of the Rift Valley, Kenya. Journal of Human Evolution 7, 101–109.

Raghavan, M., DeGiorgio, M., Albrechtsen, A., Moltke, I., Skoglund, P., Korneliussen, T.S., Grønnow, B., Appelt, M., Gulløv, H.C., Friesen, T.M., Fitzhugh, W., Malmström, H., Rasmussen, S., Olsen, J., Melchior, L., Fuller, B.T., Fahrni, S.M., Stafford, T., Grimes, V., Renouf, M.A.P., Cybulski, J., Lynnerup, N., Lahr, M.M., Britton, K., Knecht, R., Arneborg, J., Metspalu, M., Cornejo, O.E., Malaspinas, A.-S., Wang, Y., Rasmussen, M., Raghavan, V., Hansen, T.V.O., Khusnutdinova, E., Pierre, T., Dneprovsky, K., Andreasen, C., Lange, H., Hayes, M.G., Coltrain, J., Spitsyn, V.A., Götherström, A., Orlando, L., Kivisild, T., Villems, R., Crawford, M.H., Nielsen, F.C., Dissing, J., Heinemeier, J., Meldgaard, M., Bustamante, C., O'Rourke, D.H., Jakobsson, M., Gilbert, M.T.P., Nielsen, R., Willerslev, E., 2014. The genetic prehistory of the New World Arctic. Science 345, 1255832.

Rak, Y., Ginzburg, A., Geffen, E., 2002. Does *Homo neanderthalensis* play a role in modern human ancestry? The mandibular evidence. American Journal of Physical Anthropology 119, 199–204.

Reyes-Centeno, H., Ghirotto, S., Détroit, F., Grimaud-Hervé, D., Barbujani, G., Harvati, K., 2014. Genomic and cranial phenotype data support multiple modern human dispersals from Africa and a southern route into Asia. Proceedings of the National Academy of Sciences USA 111, 7248–7253.

Robbins, L.H., 1974. The Lothagam site: a Late Stone Age fishing settlement in the Lake Rudolf basin. Michigan State University Museum, Kenya. East Lansing.

Robbins, L.H., 1975. Bone artefacts from the Lake Rudolf Basin, East Africa. Current Anthropology 16, 632–633.

Robbins, L.H., 2006. Lake Turkana archaeology: The Holocene. Ethnohistory 53, 71–93.

Rohlf, F.J., Slice, D.E., 1990. Extensions of the Procrustes method for the optimal superimposition of landmarks. Systematic Zoology 39, 40–59.

Rosas, A., 1992. Ontogenia y Filogenia de la Mandíbula en la Evolución de los Homínidos. Aplicación de un Modelo de Morfogénesis a las Mandíbulas Fósiles de Atapuerca. Ph.D. Dissertation, Complutense University.

Roseman, C.C., Weaver, T.D., 2004. Multivariate apportionment of global human craniometric diversity. American Journal of Physical Anthropology 125, 257–263.

Saitou, N., Nei, M., 1987. The neighbor-joining method: a new method for reconstructing phylogenetic trees. Molecular Biology and Evolution 4, 406–425.

Schlager, S., 2013. Soft-Tissue reconstruction of the human nose: population differences and sexual dimorphism, Anthropologie. Universität Freiburg, Universitätsbibliothek Freiburg, p. 24.

Schlebusch, C.M., Malmström, H., Günther, T., Sjödin, P., Coutinho, A., Edlund, H., Munters, A.R., Steyn, M., Soodyall, H., Lombard, M., Jakobsson, M., 2017. Southern African ancient genomes estimate modern human divergence to 350,000 to 260,000 years ago. Science 358, 652–655.

Schliep, K.P., 2011. Phangorn: phylogenetic analysis in R. Bioinformatics 27, 592–593.

Schwartz, G.T., Tattersall, I., 2000. The human chin revisited: what is it and who has it? Journal of Human Evolution 38, 367–409.

Simon, C., 1989. Les populations Kerma - Evolution interne et relations historiques dans le contexte Egypto-Nubiens. Archéologie du Nil Moyen 3, 139–147.

Smith, F.H., 1982. Upper Pleistocene hominid evolution in South-Central Europe: A review of the evidence and analysis of trends. Current Anthropology 23, 666–703.

Smith, H.F., 2009. Which cranial regions reflect molecular distances reliably in humans? Evidence from three-dimensional morphology. American Journal of Human Biology 21, 36–47.

Sonneville-Bordes, D., 1959. Position stratigraphique et chronologique relative des restes humains du Paléolithique Supérieur entre Loire et Pyrénées. Annales de Paléontologie. Vertébrés 45, 19–51.

Stock, J.T., Migliano, A.B., 2009. Stature, mortality, and life history among indigenous populations of the Andaman Islands, 1871-1986. Current Anthropology 50, 713–725.

Street, M., Terberger, T., Orschiedt, J., 2006. A critical review of the German Paleolithic hominin record. Journal of Human Evolution 51, 551–579.

Svoboda, A.J., 2008. The Upper Paleolithic burial area at Předmostí: ritual and taphonomy. Journal of Human Evolution 54, 15–33.

Tishkoff, S.A., Reed, F.A., Friedlaender, F.R., Ehret, C., Ranciaro, A., Froment, A., Hirbo, J.B., Awomoyi, A.A., Bodo, J.-M., Doumbo, O., Ibrahim, M., Juma, A.T., Kotze, M.J., Lema, G., Moore, J.H., Mortensen, H., Nyambo, T.B., Omar, S.A., Powell, K., Pretorius, G.S., Smith, M.W., Thera, M.A., Wambebe, C., Weber, J.L., Williams, S.M., 2009. The genetic structure and history of Africans and African Americans. Science 324, 1035–1044.

Trinkaus, E., Svoboda, J., 2006. Early Modern Human Evolution in Central Europe. Oxford University Press, New York.

Tryon, C.A., Crevecoeur, I., Faith, J.T., Ekshtain, R., Nivens, J., Patterson, D., Mbua, E.N., Spoor, F., 2015. Late Pleistocene age and archaeological context for the hominin calvaria from GvJm-22 (Lukenya Hill, Kenya). Proceedings of the National Academy of Sciences USA 112, 2682–2687.

von Cramon-Taubadel, N., 2009a. Congruence of individual cranial bone morphology and neutral molecular affinity patterns in modern humans. American Journal of Physical Anthropology 140, 205–215.

von Cramon-Taubadel, N., 2009b. Revisiting the homoiology hypothesis: the impact of phenotypic plasticity on the reconstruction of human population history from craniometric data. Journal of Human Evolution 57, 179–190.

von Cramon-Taubadel, N., 2011. Global human mandibular variation reflects differences in agricultural and hunter-gatherer subsistence strategies. Proceedings of the National Academy of Sciences USA 108, 19546–19551.

von Cramon-Taubadel, N., 2014. Evolutionary insights into global patterns of human cranial diversity: population history, climatic and dietary effects. Journal of Anthropological Sciences 92, 43–77.

Weninger, B., Joris, O., 2004. Glacial radiocarbon calibration. The CalPal Program. In: Higham, T., Ramsey, C.B., Owen, C. (Eds.), Radiocarbon and Archaeology. Proceedings of the 4th Symposium. Oxford University School Archaeology Monograph 62, Oxford, pp. 9–15.

White, T.D., Asfaw, B., DeGusta, D., Gilbert, W.H., Richards, G.D., Suwa, G., Howell, F.C., 2003. Pleistocene *Homo sapiens* from Middle Awash, Ethiopia. Nature 423, 742–747.

White, T.D., Black, T.M., Folkens, P.A., 2011. Human Osteology Third Edition. Academic Press, Oxford.

Zaidi, A.A., Mattern, B.C., Claes, P., McEcoy, B., Hughes, C., Shriver, M.D., 2017. Investigating the case of human nose shape and climate adaptation. PLoS Genet. 13, e1006616.